AD_____

Award Number: DAMD17-02-1-0555

TITLE: Summer Undergraduate Training Program in Breast Cancer Research

PRINCIPAL INVESTIGATOR: G. Marc Loudon, Ph.D.
David Riese. Ph.D.

CONTRACTING ORGANIZATION: Purdue University
West Lafayette, IN 47907-1063

REPORT DATE: May 2005

TYPE OF REPORT: Annual Summary

PREPARED FOR: U.S. Army Medical Research and Materiel Command
Fort Detrick, Maryland 21702-5012

REPORT DOCUMENTATION PAGE

Form Approved
OMB No. 0704-0188

1. REPORT DATE *(DD-MM-YYYY)*	2. REPORT TYPE	3. DATES COVERED *(From - To)*
01-05-2005	Annual Summary	1 May 2004 - 30 Apr 2005

4. TITLE AND SUBTITLE
Summer Undergraduate Training Program in Breast Cancer

5a. CONTRACT NUMBER

5b. GRANT NUMBER
DAMD17-02-1-0555

5c. PROGRAM ELEMENT NUMBER

6. AUTHOR(S)
G. Marc Loudon, Ph.D.
David Riese. Ph.D.

5d. PROJECT NUMBER

5e. TASK NUMBER

5f. WORK UNIT NUMBER

7. PERFORMING ORGANIZATION NAME(S) AND ADDRESS(ES)
Purdue University
West Lafayette, IN
47907-1063

8. PERFORMING ORGANIZATION REPORT NUMBER

9. SPONSORING / MONITORING AGENCY NAME(S) AND ADDRESS(ES)
U.S. Army Medical Research and Materiel Command
Fort Detrick, Maryland 21702-5012

10. SPONSOR/MONITOR'S ACRONYM(S)

11. SPONSOR/MONITOR'S REPORT NUMBER(S)

12. DISTRIBUTION / AVAILABILITY STATEMENT
Approved for Public Release; Distribution Unlimited

13. SUPPLEMENTARY NOTES

14. ABSTRACT

Abstract is on page 4 of the report.

15. SUBJECT TERMS
Breast Cancer

16. SECURITY CLASSIFICATION OF:			17. LIMITATION OF ABSTRACT	18. NUMBER OF PAGES	19a. NAME OF RESPONSIBLE PERSON
a. REPORT	b. ABSTRACT	c. THIS PAGE			19b. TELEPHONE NUMBER *(include area code)*
U	U	U	UU	30	

Table of Contents

Abstract

Year 03 of the Undergraduate Training Program in Breast Cancer Research has been completed successfully. In addition to the eight students funded by this grant, two additional students were recruited and funded by the Dean of Pharmacy. Nine different mentors were involved. In the two years of the program thus far, 13 of the 22 participants have been women, who are underrepresented in the biomedical research community. Students carried out research in their mentors' laboratories, attended a weekly journal club, attended a weekly seminar of guest speakers, presented a formal oral report on their work, and wrote a final report. Three grant submissions, one pending and two funded, have resulted in part from work sponsored by this program. Participants have been listed as coauthors thus far on two presentations at meetings. Two program participants thus far are enrolled in graduate school in the life sciences.

Introduction

This report describes progress in implementing the third year of a three-year summer undergraduate training program (that has been extended to four years) in breast cancer research at Purdue University in the School of Pharmacy & Pharmaceutical Sciences and the School of Veterinary Medicine.

Body of Report

Task 1: Publicity and Notification. We contacted a number of small colleges in the vicinity of Purdue and solicited applications to the Breast Cancer Program. In addition, professional students in the Purdue Schools of Pharmacy and Veterinary Medicine were notified both by a web site and by direct class visitations. We also posted the program applications on our undergraduate research web site. We felt that the best possibility of recruiting minority students was to coordinate our efforts with those of the MARC-AIM program at Purdue.

Task 2: Schedule Seminar Speakers. Speakers were scheduled for a weekly seminar in Breast Cancer Research. For these seminars, faculty participating in the program gave talks directed to the undergraduate researchers about their research relevant to breast cancer research. In addition, a special seminar was presented by Prof. Ken Nephew, Indiana University, Bloomington, Department of Medical Sciences.

Task 3: Mail Publicity and Mount Web Site. (See also Task 1.) We agreed to allow minority applicants to take part in the MARC-AIM program. Unfortunately, no MARC-AIM applicants expressed interest in the program. One offer was made to a minority applicant who declined the offer. As noted in Task 1, applications were made available through the Undergraduate Research Web Site.

Task 4: Accept and Review Applications. Applications were accepted through February 13, 2004. As was the case in Year 02 of the program, our office was operating a more general undergraduate research program with about the same application deadlines. This program was funded by the Office of the Dean of the School of Pharmacy. This year the Dean's Program funded two additional positions. In other words, the Army grant funded eight positions, and the School funded two. *Over the past three years, the Army grant has leveraged support from other sources for a total of eight additional undergraduate research opportunities* beyond the 24 supported on this grant.

Task 5: Make Offers to Students. Prof. Riese (the co-PI) and the PI, with consultation by other participating faculty, made offers to students in mid-March. We had no indication of interest by students from the MARC-AIM program. Despite out disappointing results with minority students, it should be pointed out that 20 of the 32 participants to date have been women, which are underrepresented in the research community. The high percentage of qualified women in the Purdue Pharmacy Program (about 65%) provide fertile ground for recruiting women researchers.

Task 6a: Assign Students to Laboratories of Program Staff. This assignment was made at the time of offer; that is, students were informed with whom they would work.

Task 6b: Coordinate Assignment of Students with MARC/AIM Program. Because we had no indications in interest from MARC-AIM students, this task was not applicable.

Task 7: Complete Program Setup Tasks. Program setup tasks were accomplished prior to the start of the program on June 1.

Task 8: Preside over First Week of Program. An official meeting of students was held on June 1, 2004. Students who had not already done so were briefed on expectations for safety, seminar attendance, and reports. A barbecue was held at the home of the PI later in the summer.

Task 9: Conduct Program. The program was conducted in the manner described in the proposal. Students took part in a weekly journal club, a weekly seminar by a guest speaker, and in weekly laboratory meetings. Prof. Ken Nephew, Indiana University, Bloomington, Department of Medical Sciences, delivered the guest lecture on the role of estrogen receptor degradation in breast cancer.

Tasks 10 & 11: Final Reports. Students were scheduled about one month in advance for their final reports, and a letter was sent to each describing expectations for their final written report. Each student presented a 15-minute PowerPoint seminar describing his/her work in a public seminar. Each student also provided the PI and Prof. Riese with a short report summarizing their research and evaluating the program in answer to specific questions. Summaries of the research conducted by each student are provided at the end of this report.

Task 12: Review Students' and Members Final Reports. Student final reports were due, and were received, on or before September 1, 2004.

Task 13: Survey Students about Attitudes and Career Choices. As part of the summary report, students were asked about their attitudes toward research, and whether they were contemplating a career path in research.

Task 14: Make Yearly Report to Breast Cancer Program. This report fulfills this task.

Summary Reports of Key Research Accomplishments

Names of Students, Home Institutions, and Mentors

Katherine E. Behr (Purdue University School of Pharmacy), Prof. Ross Weatherman
John Bossaer (Purdue University School of Pharmacy), Prof. Robert Geahlen
Lauren Carlson (Purdue University School of Pharmacy), Prof. Mark Cushman
Jonathan Hoggatt (Purdue University Pharmaceutical Sciences), Prof. Richard Gibbs
Rachel Fry (Purdue University School of Pharmacy), Prof. David Riese
Dania Jaara (Purdue Biology), Prof. Sophie LeLievre
Grace O'Connor (Purdue University School of Pharmacy), Prof. Suresh Mittal
Netty Santoso (Purdue University Pharmaceutical Sciences), Prof. Dai Sakamuro
Jing Tan (Purdue University Prepharmacy), Prof. Richard Gibbs
Zachary Weber (Purdue University School of Pharmacy), Prof. Shuang Liu

Reports of Students' Accomplishments
(These reports were provided by the students themselves with minor edits.)

Katherine E. Behr. This summer I had the opportunity to work closely with Dr. Ross Weatherman and his lab conducting experiments on tamoxifen and its effects on estrogen receptors. The goal of my project was to synthesize endoxifen, the major metabolite of tamoxifen, using a scheme developed by the lab. If I completed this project, then I could expand and create multiple analogs of endoxifen using different reactants and schemes. To synthesize

endoxifen, I used a scheme of four reactions. I began by adding β-bromophenotole, dichloromethane, and *p*-anisoyl chloride using a Friedel-Crafts acylation reaction. After this reacted overnight, I conducted a McMurray coupling by adding the product to a $Zn/TiCl_4$ complex and propiophenone. Next, I synthesized methoxyendoxifen using an S_N2 reaction by adding the McMurray product to CH_3NH_2 and allowing the mixture to react overnight in a sealed high-pressure flask. Lastly, I deprotected this product using L-selectride to obtain my final product of endoxifen. Since I completed this scheme in two weeks, I was free to synthesize other analogs using various methods. During my fellowship I created didesmethyltamoxifen, fluoresceine tamoxifen conjugates #1 and #2, Boc-protected linker tamoxifen, as well as half the reactions needed to form GW7604. These compounds will be used on breast cancer cells to determine their method of action and if any are more useful than tamoxifen. The compound GW7604 is of special interest because of its antiestrogenic properties in the breast as well as uterus, unlike tamoxifen which has estrogenic effects in the uterus, placing patients at higher risk for endometrial cancers.

John Bossaer. *Syk* is a non-receptor protein tyrosine kinase that is normally expressed in hematopoietic cells. It also has been found in cells of epithelial (i.e. breast) origin. However, *syk* expression is absent or reduced in highly malignant and invasive tumors. It is thought that *syk* may somehow serve as a tumor suppressor, possibly by promoting apoptosis. One hallmark of cancer cells is the ability to avoid apoptosis. This evasion process leads to the fixation of mutations undergone during normal events of the cell cycle that would normally either be fixed or result in apoptosis of the cell. These mutations in turn can further advance the malignancy of the cell by making it grow self sufficiently or make it resistant to growth inhibitory stimuli. I induced apoptosis using Tumor Necrosis Factor (TNF) in MCF-7 breast cancer cells transfected with *syk* fluorescently tagged or a negative fluorescent control. Cells were then stained with Annexin V to visualize apoptosis. At this time *syk*'s possible role in apoptosis is unclear.

Lauren Carlson. The goal of my project this summer was to create a bis-indenoisoquinoline with a benzene ring between the amino groups and 3-carbon chains connecting the amino groups to the indenoisoquinoline structure (bis-{(5,6-dihydro-5,11-diketo-11*H*-indeno[1,2-*c*]isoquinoline)-6-propylamino}-1,3-phenylenediamine). Since a recently developed bis-indenoisoquinoline (NSC 727357) had been produced that showed very high cytotoxity in cancer cells, we wanted to model my structure after it and place the benzene ring in the middle with hopes of restricting its conformation. This would allow observations to be made as to how conformation affects a bis-indenoisoquinoline's activity in a cancer cell. The product was synthesized, purified, and crystallized after many attempts and revision of synthesis schemes. An NMR spectrum of the product, unfortunately, was somewhat confusing. The protons from the side chains were all accounted for, but a few protons appeared to be missing from the aromatic proton peaks. The NMR spectrum was compared to that of NSC 727357, and from the data, it was assumed that the aromatic protons from the benzene ring in the middle appear to be missing. The results from the mass spectrometry test did indeed have a peak at the desired molecular weight, but it wasn't the most prevalent peak in the sample. Nothing more was done with this compound, but implementation of ideas for how to fine-tune the reaction in order to get the final product is underway.

Jonathan Hoggatt. My project involved developing a mass spectrometric technique for the detection of post-translational farnesylation of *ras* proteins. Mutated *ras* proteins have been found in approximately 30% of all human cancers and thus present themselves as a possible target for anticancer agent development. Mutated *ras* lacks normal GTPase activity, and thus is in a constantly active state. This constant activation causes continuous cell proliferation and

tumor growth. *Ras* must be localized on the cellular membrane to be active and localization is achieved through the post-translational addition of a farnesyl group to the carboxy terminus cysteine residue. Inhibition of farnesylation or alternate farnesylation through farnesyl analogs may prevent membrane localization and thus inhibit the function of mutated *ras*. A mass spectrometric technique is needed to detect what farnesylation reactions have occurred in various cellular models to work in conjunction with studies currently underway to develop competing farnesyl analogs.

Rachel Fry. My summer research project focused on the ErbB4 receptor, which is a member of the ErbB family of tyrosine kinases. Overexpression of other ErbB members: ErbB1, ErbB2, and ErbB3, correlates with tumor aggressiveness and a poor breast cancer prognosis. Overexpression of ErbB4, however, correlates with less aggressive tumors and increased survival. Early studies involving constitutively active ErbB4 homodimers have linked ErbB4 expression with growth inhibition of breast and prostate cancer cells. Other studies involving various ErbB4 mutants have shown the tyrosine 1056 (Y1056) in the terminal domain may be necessary and sufficient to couple to this growth inhibition. While these findings are early and many more studies are needed, the ErbB4 receptor may play an important role in breast cancer research and may act as a prognosis tool in the future.

My research project focused on the ErbB4 receptor and Y1056. I worked on making a vector containing a GST-tagged portion of the terminal domain of the ErbB4 receptor containing the Y1056 residue. Once completed, this vector was to be transfected into a S2 cell line and expression induced. The ErbB4 would be purified from the media using a GST column and at least one mutant of Y1056 would be made. The mutant would contain a glutamic acid, which is a phosphorylated tyrosine residue mimic at this site, and the control would have an unphosphorylated tyrosine. Cell lysate would then be bound to these two ErbB4 proteins and analyzed by SDS-PAGE. The result would be analyzed by identifying with cell lysate proteins coupled to the glutamic acid but did not bind to the unphosphorylated tyrosine. Using these glutamic acid bound proteins, a possible signaling pathway coupling ErbB4 expression to its growth inhibition effect could be studied. Unfortunately, this project was not completely accomplished during the summer, but I will continue working on it and it will hopefully be completed during the school year with further research.

Dania Jaara. The hypothesis of our summer project was that non-neoplastic breast epithelial cells promote breast tumor progression by enhancing the proliferation and/or by reducing the apoptosis of malignant epithelial cells. We used genetically-related neoplastic (T4-2) and non-neoplastic breast epithelial cells (S1). In a three-dimensional (3D) cell culture S1 cells grow into tissue-like glandular structures (S1-acini) whereas the T4-2 cells develop into tumor nodules. A trans-well 3D co-culture of S1-acini and T4-2 malignant cells was set up using porous membrane filters. This condition allows the transfer of diffusible factors between the two cell populations. In the presence of S1-acini, the T4-2 cells formed a significantly higher number of tumor clusters than when they were cultured alone. This effect was found to be due to reduced apoptosis (measured by TUNEL) of T4-2 cells in the co-culture. There was no effect on proliferation rate as measured by Ki-67. A cytokine array showed interesting differences including a remarkable down-regulation of IL-6 in conditioned medium obtained from T4-2-S1 coculture, suggesting that indeed the coculture influences the secretion of paracrine factors. The preliminary data suggest that non-neoplastic breast epithelial cells may promote the survival of malignant epithelial cells through diffusible factors. This effect may promote early breast tumor progression where the survival of malignant cells is particularly crucial.

Grace O'Connor. EphA2 is a receptor tyrosine kinase that is normally present in relatively low concentrations on adult epithelial mammary cells. When it binds to its ligand, EphrinA1, it is autophosphorlyated; this overphosphorylation is necessary for normal cell function. In many of the most aggressive breast cancers, EphA2 is overexpressed, but does not bind to EphrinA1 and get phosphorlyated; this causes even more accumulation in the cell. The hypothesis was that overexpression of EphA2 by infection with HAdEphA2 (replication deficient adenoviral vector with EphA2 gene insert) in MDA-MB231 (human breast cancer) cells will lead to increased EphA2 phosphorylation, decreased colony growth in soft agar assay, and decreased viability. Last year, I showed with Western blots that treating MDA-MB231 cells with HAdEphA2 increases EphA2 phosphorylation to levels similar to MCF-10A (normal human breast cells). This year, I also did Western blots for different proteins, such as EphrinA1, CoxII, PARP, pAKT, and Fibronectin. However, the HAdEphA2 treatment had little or no effect on the expression levels of these proteins compared to HAdΔE1,E3 (adenoviral vector with no insert). For the soft agar assay, the HAdEphA2 treated MDA-MB231 cells actually formed a statistically significant higher number of colonies compared to the HAdΔE1,E3 or mock (PBS) treated. Additionally, there was no significant difference in the viability of the HAdEphA2 group compared to HAdΔE1,E3. It is not clear why HAdEphA2 infection increases phosphorylation in MDA-MB231 cells, but does not seem to have an effect on other things.

Netty Santoso. This summer I work primarily with BIN1. BIN1 is a novel tumor suppressor protein, whose expression is widely reduced or lost in breast, liver, and prostate cancer cells. BIN1 interacts with *N*-terminus of *c-myc* oncoprotein, and inhibits *c-myc* dependent cellular transformations. BIN1 is normally ubiquitous in any cells, but interestingly MCF7 breast cancer cells do not express BIN1 protein. Therefore, we investigated the role of BIN1 protein in MCF7 breast cancer cell line. We performed colony formation assays to check tumor suppressive activity of BIN1 in MCF7 cell line. MCF7 cells were transfected with BIN1 and pCDNA3 (vector control), BIN1-transfected cells formed significantly less colonies than pCDNA3-transfected cells. These observations suggest that BIN1 protein has tumor suppressive activity in MCF7 breast cancer cells. In the future, we are interested to develop a drug that can activate the expression of BIN1 protein in breast cancer cells. To better understand BIN1-dependent multiple tumor suppressor target, we identified BIN1-interacting protein. From GST pull-down assay, we were able to detect BIN1-interacting proteins with sizes around 53 kDa and 160 kDa. These BIN1 specific-interacting proteins should be analyzed further by mass spectrometry to obtain the amino acid sequences.

Jin Tan. *Ras* protein is a key signal transduction protein and involved in cell proliferation and survival. *Ras* proteins are synthesized biologically from inactive precursor molecules in the cytoplasm. These precursor molecules of *ras* protein experience multiple post-translational modifications before they become mature. Farnesylation by farnesyltransferase (FTase) is a key event in membrane localization, so farnesyltransferase inhibitors (FTIs) have considerable promise as agents to treat breast cancer. The membrane localization of *ras* is blocked by FTIs. In the summer research program, my major work was to synthesize some 3-substituted FPP analogues, which will be evaluated as inhibitors by graduate students in the Gibbs lab. During this summer, I have synthesized two 3-substituted FPP analogues through copper-mediated coupling of a vinyl triflate with various Grignard reagents. These two compounds are 3-propyl FPP and 3-ethyl FPP. In the near future, other students will continue synthesizing more 3-substituted FPP and analyzing their properties.

Zachary Weber. The basis of my summer research was the synthesis of peptides that could potentially be used in the imaging of breast tumors. These peptides, which are called cyclic

RGD peptides (because of their arginyl-aspartyl-glycine motif), are targeted to bind to $\alpha_v\beta_3$ integrin receptors. These receptors are overexpressed on tumor neovasculature and on tumor cells themselves. The increased presence of integrin receptors is therefore an intriguing target for new imaging agents, and specifically for breast tumor imaging. The cyclic RGD peptides that I synthesized were composed of four main components; a targeting biomolecule, linker, bifunctional chelator, and radionuclide. The final molecule was then made by a series of reactions to combine each of these parts. The first step was to protect the *N*-terminus of an amino acid linker with a Boc group. Once protected, activated esters sites were formed at which the targeting biomolecule then bonded to the linker. After adding the targeting biomolecule, the Boc group was removed and a bifunctional chelator was added that eventually bonded to a radionuclide. The goal of developing these molecules is to provide earlier and more accurate detection of breast tumors. This superior diagnosis will be based upon the receptor-specific uptake of the peptides and will hopefully provide a clearer image of breast tissue and potential breast cancer.

Reportable Outcomes

- Ten undergraduate students, each working with one of nine mentors, carried out breast cancer research in the Summer of 2004, bringing the total number of students sponsored by the program over three years to 32.
- Two of the students were supported by the Office of the Dean of Pharmacy.
- All students provided favorable reviews of the program.
- Of the 32 participants for the first two years, 20 have been women. Women are underrepresented in the life science academic and research community.
- A funded grant application has resulted in part from the work of one participant (Marintha Meckley, Year 01):

  Title of Grant: *Novel Indenoisoquinoline Topoisomerase I Inhibitors*
  Principal Investigator: Prof. Mark Cushman
  Grant Number: NIH R01 CA089566
  Term: 07/01/5005-6/30/2010
  Current Year Direct Cost: $250,000

- One grant application (not yet funded) has been based in part on the work carried out by Marygrace Foster and Joshua McAfee (Year 02 participants) and John Bossaer (a Year 03 participant):

  Title:of Grant: *Syk and Associated Proteins in Breast Cancer*
  Principal Investigator: Prof. Robert. L. Geahlen
  Agency: NIH/NCI
  Year 1 DC requested:: 225,000; TC: 329,520

- Two published papers have also resulted from the work of participants in the program. (Others were reported last year.) The names of the participants are bolded and the year in the program are added in parentheses:

  M. Nagarajan, A. Morrell, B. C. Fort, **M. R. Meckley (01)**, S. Antony, G. Kohlhagen, Y. Pommier, and M. Cushman, "Synthesis and Anticancer Activity of Simplified Indenoisoquinoline Topoisomerase I Inhibitors Lacking Substitutions on the Aromatic Rings," J. Med. Chem. **47**, 5651-5661 (2004)

E.E.Williams, (02)., **L.J. Trout (01)**, R.M. Gallo, S.E. Pitfield, D.J. Penington, I. Bryant, and D.J. Riese II., "A constitutively-active ErbB4 mutant inhibits drug-resistant colony formation by the DU-145 and PC-3 human prostate tumor cell lines." *Cancer Letters* **192** 67-74 (2003).

A PDF copy of each paper has been submitted with this report.

- Several meeting presentations have resulted from the work of program participants:

Bryant, I., **E.E. Williams (02)**, **L.J. Trout (01)**, S. Pitfield, S. Shukla, J. Martin, R.M. Gallo, D.J. Penington, and D.J. Riese II. "A Constitutively Active ErbB4 Mutant Inhibits Colony Formation by Human Breast and Prostate Cell Lines." Tyrosine Phosphorylation and Signal Transduction Meeting, Salk Institute, La Jolla, CA, August 2002.

Penington, D.J., **E.E. Williams (02)**, S.S. Hobbs, J. Vanderpoel, R.M. Gallo, S. Slavik, E.M. Cameron, I. Bryant, A.T.D. Le, E.N. Blommel, S. Shukla, R.P. Hammer, V.J. Watts, and D.J. Riese II. "Multifaceted Approach to Study and to Target ErbB Family Receptor Signaling and Coupling to Biological Responses." Era of Hope Meeting, Orlando, FL, September 2002.

Williams, E.E. (02), I. Bryant, S. Slavik, S. Shukla, J. Martin, D.J. Penington, and D.J. Riese II. "A Constitutively-Active ErbB4 Mutant Inhibits Colony Formation by Human Breast and Prostate Cell Lines." Era of Hope Meeting, Orlando, FL, September 2002.

Hobbs, S.S., E.M. Cameron, R.P. Hammer, A.T.D. Le, **E.E. Williams (02)**, R.M. Gallo, E.N. Blommel, S.L. Coffing, H. Chang, and D.J. Riese II. "The Basis of ErbB4 Ligand Specificity." Nineteenth Annual Meeting On Oncogenes, Hood College, Frederick, MD, June 2003.

Pitfield, S.E., **E.E Williams (02), L.J. Trout (01),** R.M. Gallo, I. Bryant, D.J. Penington and D.J. Riese II. "A Constitutively Active ErbB4 Mutant Inhibits Drug-Resistant Colony Formation By Human Breast and Prostate Cell Lines." Nineteenth Annual Meeting On Oncogenes, Hood College, Frederick, MD, June 2003.

- Professor David Riese II, the co-PI of this grant, will be attending the 4th Era of Hope meeting, to be held June 8–11, 2005, in Philadelphia, Pennsylvania.
- As noted in last year's report, unused travel funds have been rebudgeted for student support and a one-year no-cost extension of this grant has been obtained. This will allow us to offer this program for an additional year, and this final year (04) is in progress now.

Synthesis and Anticancer Activity of Simplified Indenoisoquinoline Topoisomerase I Inhibitors Lacking Substituents on the Aromatic Rings

Muthukaman Nagarajan,† Andrew Morrell,† Brian C. Fort,† Marintha Rae Meckley,† Smitha Antony,‡ Glenda Kohlhagen,‡ Yves Pommier,‡ and Mark Cushman*,†

Department of Medicinal Chemistry and Molecular Pharmacology, School of Pharmacy and Pharmacal Sciences, Purdue University, West Lafayette, Indiana 47907, and Laboratory of Molecular Pharmacology, Center for Cancer Research, National Cancer Institute, Bethesda, Maryland 20892-4255

Received February 3, 2004

The indenoisoquinolines are a class of cytotoxic topoisomerase I inhibitors that offer certain advantages over the camptothecins, including the greater stabilities of the compounds themselves, as well as the greater stabilities of their drug–enzyme–DNA cleavage complexes. To investigate the possible biological roles of the di(methoxy) and methylenedioxy substituents present on the aromatic rings of the previously synthesized indenoisoquinoline topoisomerase I inhibitors, a series of compounds lacking these substituents was synthesized and tested for both cytotoxicity in cancer cell cultures and for enzyme inhibitory activity. The results indicate that the aromatic substituents make a small, but consistently observable contribution to the biological activity. Molecular models derived for the binding of the unsubstituted indenoisoquinolines in ternary complex with DNA and topoisomerase I indicate that the substituents on the lactam nitrogen project out of the major groove, and the carbonyl group is directed out of the minor groove, where it is involved in a hydrogen bonding interaction with the side chain guanidine group of Arg364. The DNA cleavage patterns observed in the presence of topoisomerase I and various indenoisoquinolines were similar, although significant differences were detected. There were also variations in the DNA cleavage pattern seen with camptothecin vs the indenoisoquinolines, which indicates that these two classes of topoisomerase I inhibitors are likely to target the cancer cell genome differently, resulting in different spectra of anticancer activity. The most cytotoxic of the presently synthesized indenoisoquinolines has a 4-amino-*n*-butyl group on the lactam nitrogen.

Introduction

The topoisomerase I (top1) inhibitory activity of NSC 314622 (**1**)[1] was discovered after a COMPARE analysis of its cytotoxicity profile revealed a strong resemblance to that of other known top1 inhibitors, including camptothecin (**2**) and the clinically useful anticancer drug topotecan (**3**).[2] The indenoisoquinoline **1**, like **2** and **3**, stabilizes DNA-top1 cleavage complexes by intercalating at the DNA cleavage site, resulting in inhibition of the religation reaction.[2–4] These inhibitors are therefore classified as top1 "poisons" as opposed to top1 "suppressors", which inhibit the DNA cleavage reaction. However, there are differences in the biological activities of NSC 314622 (**1**) in comparison with camptothecin (**2**) and the clinically useful anticancer drugs topotecan (**3**) and irinotecan (**4**) that warrant further development of the indenoisoquinolines. First, the DNA cleavage site specificity of **1** is different from that of camptothecin (**2**), so different genes could be targeted and provide a different antitumor spectrum.[2] The cytotoxic activity of topoisomerase inhibitors is indeed dependent on the production of DNA breaks, which inhibit (damage) certain regions of the genome in a sequence-specific or sequence-dependent manner, and which activate death response pathways by forming irreparable DNA lesions and/or inducing apoptosis. It is known that the clinically useful topoisomerase II (top2) inhibitors have preferential activity for different cancers, and it can be expected that different top1 inhibitors will display different spectra of anticancer activity as well.[5] Second, the cleavage complexes induced by the indenoisoquinoline **1** are more stable than those formed in the presence

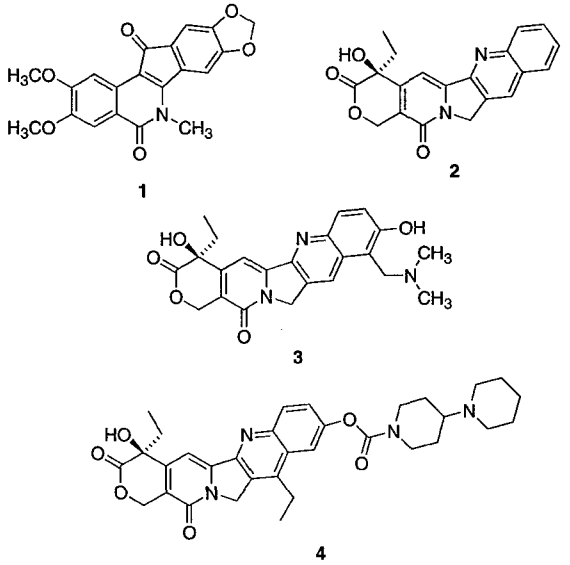

1 2 3 4

* To whom correspondence should be addressed: Tel: 765-494-1465. Fax: 765-494-6790. E-mail: cushman@pharmacy.purdue.edu.
† Purdue University.
‡ NIH, Bethesda, MD.

10.1021/jm040025z CCC: $27.50
Published on Web 10/02/2004

of camptothecin (**2**).[2] The reversibility of camptothecin-induced cleavage complexes imposes long infusion times for maximum activity, so noncamptothecin topl inhibitors with enhanced cleavage complex stabilities may offer the advantage of shorter administration times.[6] For the camptothecins, SN-38 produces more stable cleavage complexes and is also more active as an antitumor agent in tumor models. Third, the camptothecins, in contrast to the indenoisoquinolines, are chemically unstable due to lactone ring opening to form an inactive hydroxy acid.[7] The lactone is in equilibrium with the hydroxy acid, but the equilibrium is shifted toward the inactive hydroxy acid as the carboxylate of the ring-open form binds tightly to serum albumin. Although these reasons recommend the further development of the topl inhibitor NSC 314622 (**1**) as an anticancer agent, the usefulness of compound **1** itself is limited by its moderate potency, both as a cytotoxic agent in cancer cells and as a topl inhibitor.[8] Therefore, a number of additional indenoisoquinolines related to **1** have been synthesized and evaluated, with most of the more active compounds having di(methoxy) or methylenedioxy substituents on the two aromatic rings.[8–11]

The present investigation was undertaken in order to determine whether a simplified system lacking the usual di(methoxy) and methylenedioxy substituents on the two aromatic rings of the indenoisoquinoline system could retain significant cytotoxicity and topl inhibitory activity. A limited number of compounds fitting this description were reported early on, and they were found to be generally less active than the parent compound **1**, or to have comparably moderate activity.[8,12] In the meantime, several developments have occurred that have led to a reinvestigation of the series of compounds lacking aromatic substituents. A crystal structure of an intercalation complex containing topotecan (**3**), human topl, and duplex DNA has been reported.[4] Models of various indenoisoquinolines in ternary complex with topl and cleaved duplex DNA have been generated using the reported coordinates of the topotecan complex, assuming that the lactam rings of both systems are oriented similarly in their cleavage complexes.[11] These models do not suggest any critical role of the substituents on the two aromatic rings of the indenoisoquinolines that would preclude binding of their unsubstituted analogues. An additional development is that a number of indenoisoquinolines have been synthesized that contain aminoalkyl substituents on the lactam nitrogen, and some of these compounds have displayed topl inhibitory activity commensurate with that of camptothecin. In addition, they are very cytotoxic in cancer cells. For example, the indenoisoquinoline **5**, also known as MJ-III-65 or NSC 706744, has a mean-graph midpoint in the NCI cytotoxicity screen of 0.11 μM.[9] Furthermore, the rate constant for cleavage complex reversal with indenoisoquinoline **5** was recently determined to be about one-fourth that of camptothecin at 25 °C, while the rate constant for cleavage complex formation with **5** was approximately twice that of camptothecin.[13] Compound **5** also displayed activity vs camptothecin-resistant topoisomerases I.[13] The results suggest that the simplified indenoisoquinolines lacking aromatic substituents could hypothetically be potent topl inhibitors and cytotoxic agents if the right substitutions were made on the lactam nitrogen. This hypothesis is also supported by the antineoplastic activity reported for oracin (**6**), which has been reported to induce G2 cell cycle arrest and apoptosis in Burkitt's lymphoma cells.[14–19]

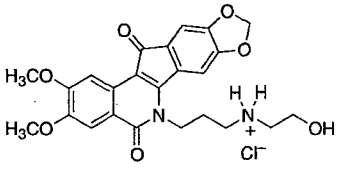

5

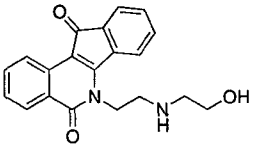

6

Chemistry

The indenoisoquinolines **8**–**22** were synthesized directly or indirectly by reacting commercially available benz[*d*]indeno[1,2-*b*]pyran-5,11-dione (**7**) with various primary amines as outlined in Scheme 1. Treatment of chloroform solutions of the BOC-protected amines **8**, **12**, and **21** with hydrochloric acid in ether resulted in their conversions to the deprotected amine hydrochlorides **9**, **13**, and **22**, respectively. The guanidine trifluoroacetate derivative **15** resulted from treatment of the free base **14** with 1,3-bis(*tert*-butoxycarbonyl)-2-methyl-2-pseudourea and mercuric chloride in aqueous THF, followed by trifluoroacetic acid. The bromide **18**[9] was obtained along with the triethylammonium salt **19** after reaction of **7** with bromopropylamine hydrobromide and triethylamine in chloroform. A nucleophilic displacement reaction between the bromide **18**[9] and 1-(3-aminopropyl)-imidazole yielded the expected product, which was isolated as the di(hydrochloride) salt **20**. The remaining products displayed in Scheme 1 were obtained directly through treatment of lactone **7** with the required primary amines.

Three indenoisoquinolines **31**, **32**, and **33**, which are unsubstituted on the isoquinolone part of the indenoisoquinoline ring system, but substituted with methylenedioxy on the indenone moiety, were obtained as outlined in Scheme 2. This synthesis relies on the condensation of Schiff bases with homophthalic anhydrides as the key step to afford substituted isoquinolines.[20] Treatment of piperonal (**23**) with ethylamine, propylamine, or 3-bromopropylamine afforded the corresponding Schiff bases **24**, **25**, and **26**, which were reacted with homophthalic anhydride (**27**) to afford the substituted isoquinolones **28**, **29**, and **30**. The 6–7 Hz coupling constant observed for the two methine protons in the ^{1}H NMR spectra of the products **28**–**30** is consistent with the assigned cis stereochemistry.[21] In contrast, these two protons usually appear as broad singlets in the ^{1}H NMR spectra of the trans diastereomers in closely related systems.[21] The (methylenedioxy)phenyl ring and the carboxyl group are both pseudoaxial due to $A^{(1,2)}$ strain in the trans diastereomers, involving a nonbonded interaction between the *N*-alkyl and the adjacent phenyl substituents, which results in both methine protons being predominantly pseudoequatorial.[22,23] In the cis diastereomers, one pseudoaxial proton (most likely at C-4) and one pseudoequatorial proton (most likely at C-3) are present. The desired indenoisoquinolines **31**, **32**, and **33** were obtained after treatment of **28**, **29**, and **30** with thionyl

Scheme 1

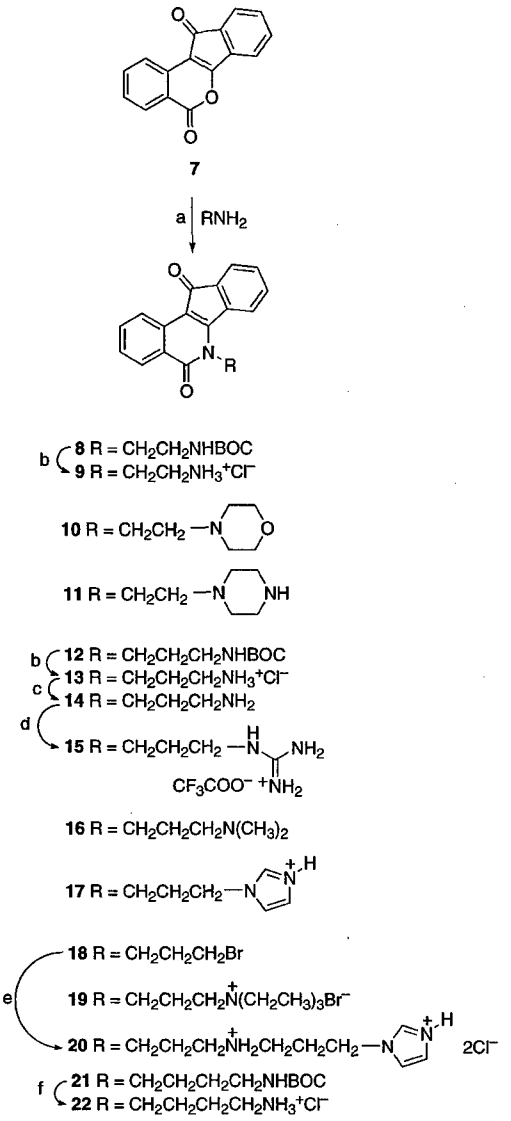

[a] Reagents and conditions: (a) $CHCl_3$, 23 °C; (b) HCl, $CHCl_3$, Et_2O, 23 °C (72 h); (c) NaOH, Et_2O; (d) 1,3-bis(*tert*-butoxycarbonyl)-2-methyl-2-pseudourea, $HgCl_2$, THF, 50 °C (2 h), 23 °C (5 h); (e) 1-(3-aminopropyl)imidazole, K_2CO_3, 1,4-dioxane, 100 °C (4 h); (f) HCl, $CHCl_3$, Et_2O, 23 °C (5 h).

chloride.[1] Nucleophilic displacement of the bromide from **33** with azide afforded intermediate **34**, which was converted to the amine using the Staudinger reduction.[24] The amine was isolated as its hydrochloride salt **35**.

Biological Results and Discussion

The indenoisoquinolines were examined for antiproliferative activity against the human cancer cell lines in the National Cancer Institute screen, in which the activity of each compound was evaluated with approximately 55 different cancer cell lines of diverse tumor origins. The GI_{50} values obtained with selected cell lines, along with the mean graph midpoint (MGM) values, are summarized in Table 1. The MGM is based on a calculation of the average GI_{50} for all of the cell lines tested (approximately 55) in which GI_{50} values below and above the test range (10^{-8} to 10^{-4} M) are

Scheme 2

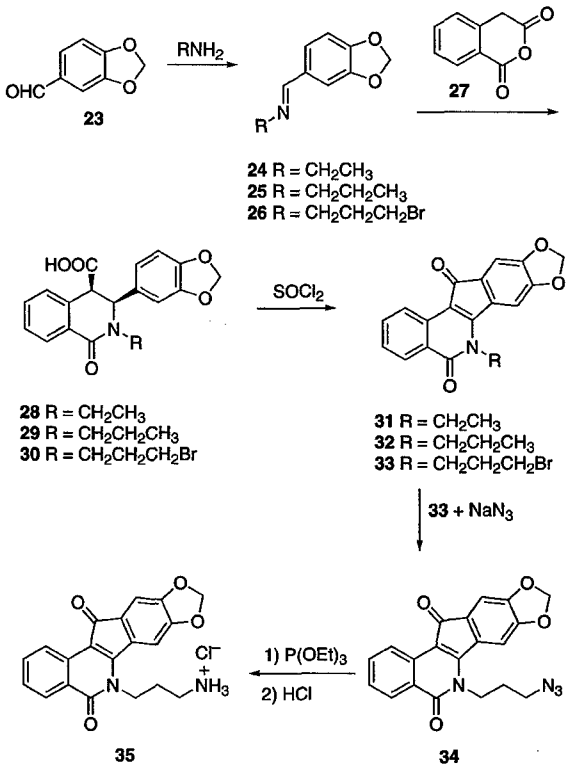

taken as the minimum (10^{-8} M) and maximum (10^{-4} M) drug concentrations used in the screening test. Therefore, the MGM value represents an overall assessment of toxicity of the compound across numerous cell lines. For comparison purposes, the activities of the previously reported lead compound **1**[8] and its more potent derivative **5**[9] are also included in the table, along with the cytotoxicity data for camptothecin (**2**). The relative potencies of the compounds in the production of topoisomerase I-mediated DNA cleavage are also listed. The activity of the compounds to produce top1-mediated DNA cleavage was expressed semiquantitatively as follows: +: weak activity; ++: similar activity as the parent compound **1**; +++ and ++++: greater activity than the parent compound **1**; ++++: similar activity as 1 μM camptothecin.

It is important to note that as an approximate average cytotoxicity, the MGM value can be misleading, because it fails to indicate the degree of selective cytotoxicity in particular cell lines. For example, it is possible that a particular drug scaffold may be highly effective for many cell lines and yet have a high MGM due to low cytotoxicity in a relatively small number of cell lines. Conversely, a particular compound may be of interest because it is highly cytotoxic in one cell line or a small number of cell lines, and still have a high MGM. Therefore, it is important to look at the individual cytotoxicity measurements for each cell line with each compound. For example, compound **15** is significantly more cytotoxic than **11** in the SN12C renal cancer cell line, yet **15** has a higher MGM value than **11** (Table 1).

Several of our previously synthesized compounds are included in Table 1 for the sake of comparison with the presently reported top1 inhibitors. These include the indenoisoquinolines **36**,[9] **37**,[9] **38**,[9] **39**,[11] **40**,[9] **41**,[9] **42**,[11] and **43**.[8] The most cytotoxic of the previously reported

Table 1. Cytotoxicities and Topoisomerase I Inhibitory Activities of Indenoisoquinoline Analogues

	cytotoxicity (GI_{50} in μM)[a]									
compd	lung HOP-62	colon HCT-116	CNSS F-539	melanoma UACC-62	ovarian OVCAR-3	renal SN12C	prostate DU-145	breast MDA-MB-435	MGM[b]	top1 cleavage[c]
1	1.3	35	41	4.2	73	68	37	96	20.0	++
2	0.01	0.03	0.01	0.01	0.22	0.02	0.01	0.04	0.0405 ± 0.0187	++++
5	0.02	0.10	0.04	0.03	0.35	>0.01	>0.01	0.79	0.11 ± 0.05	++++
6	1.62	1.12	1.65	1.42	3.85	0.95	1.28	2.56	1.90 ± 0.80	+
9	0.62	0.27	0.21	0.92	0.71	0.49	0.76	0.92	0.53 ± 0.32	+++
10	>100	36.3	85.1	29.5	81.3	93.3	>100	>100	67.6	++++
11	1.91	0.58	1.99	1.38	1.12	2.19	3.09	1.95	1.86	+
13	0.20	0.18	0.25	0.26	1.38	0.16	0.22	0.78	0.32 ± 0.23	+++
15	0.69	22.4	0.37	11.0	18.2	0.23	7.59	25.7	9.77	++++
16	1.74	0.58	1.86	0.51	1.7	0.91	1.32	2.82	1.86	+++
17	2.69	1.41	2.34	0.79	1.66	1.66	1.41	2.75	1.86	+++++
20	0.41	1.58	1.07	6.92	1.78	2.00	0.41	1.45	1.00 ± 0.31	++
22	0.08	0.10	0.10	0.05	0.52	0.04	0.01	0.84	0.16 ± 0.01	+++
31	36.3	95.5	40.7	20.0	89.1	>100	>100	>100	51.3	+++
32	>100	30.2	>100	>100	20.9	>100	>100	>100	66.1	++
33	0.69	22.4	0.37	11.0	18.2	0.23	7.59	25.7	9.77	+
35	0.28	0.68	0.43	0.18	1.45	0.19	0.06	1.82	0.25 ± 0.05	+
36	3.81	3.86	2.24	8.08	5.87	4.39	3.50	3.70	4.37 ± 0.65	±
37	5.62	4.95	12.2	18.2	74.2	16.4	16.4	76.7	14.5 ± 2.48	++
38	4.89	3.64	52.5	16.3	28.8	6.49	9.56	39.7	10.3 ± 2.56	++
39	0.58	0.068	1.3	0.14	0.86	0.36	0.40	1.04	0.34 ± 0.11	++++
40	0.19	0.35	2.93	1.27	0.85	0.43	0.89	1.05	0.62	++
41	0.06	0.13	0.26	0.25	0.31	0.31	0.04	1.21	0.16 ± 0.12	+++
42	0.018	0.12	0.19	0.54	1.4	0.9	0.14	0.65	0.35	++++
43	2.2	2.6	2.0	2.1	3.0	3.6	2.3	2.6	2.4	±

[a] The cytotoxicity GI_{50} values are the concentrations corresponding to 50% growth inhibition. [b] Mean graph midpoint for growth inhibition of all human cancer cell lines successfully tested. [c] The compounds were tested at concentrations ranging up to 10 μM. The activity of the compounds to produce top1-mediated DNA cleavage was expressed semiquantitatively as follows: +: weak activity; ++: similar activity as the parent compound **1**; +++ and ++++: greater activity than the parent compound **1**; ++++: similar activity as **1** μM camptothecin.

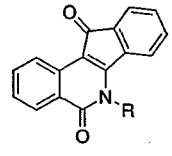

36 R = CH_2CH_2Cl
37 R = CH_2CH_2OH
38 R = $CH_2CH_2CH_2OH$

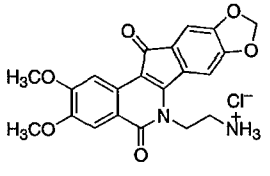

39

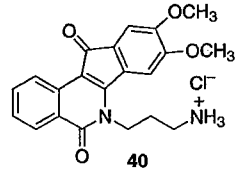

40

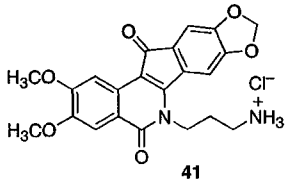

41

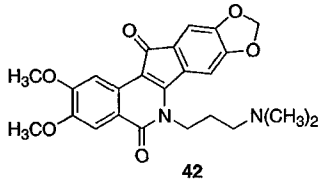

42

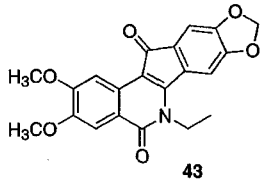

43

indenoisoquinolines lacking substituents on the two aromatic rings was compound **36**, which displayed an MGM value of 4.4 μM and a relative top1 inhibitory potency of (±) (Table 1). On the other hand, the two most potent top1 inhibitors of the previously reported indenoisoquinolines lacking substituents on the two aromatic rings were **37**, which displayed a relative potency of (++), and its higher homologue **38**, having a 3-hydroxypropyl substituent on the nitrogen, which also showed top1 inhibitory potency of (++).[12] Compounds **37** and **38** had MGMs of 14.5 μM and 10.3 μM, respectively. The two most cytotoxic of the presently synthesized indenoisoquinolines lacking aromatic substituents are **22** (MGM 0.16 μM), having a 4-amino-*n*-butyl substituent on the lactam nitrogen, and its lower homologue **13** (MGM 0.32 μM). The most potent top1 inhibitor of the new indenoisoquinolines was the 3-imidazolyl-1-propyl compound **17**, having a relative top1 inhibitory potency of (+++++). It can therefore be concluded that there is nothing inherent in the indenoisoquinolines lacking aromatic substituents that would preclude potent cytotoxicity and top1 inhibitory activity. Very cytotoxic agents and potent top1 inhibitors can be obtained provided the right substituents are present on the lactam nitrogen. However, obviously, in this particular set of indenoisoquinolines, cytotoxicity and top1 inhibitory activity are not maximized in the same compound.

The reasons for the enhanced cytotoxicities of indenoisoquinolines bearing aminoalkyl substituents are not clear. It is possible that the positively charged ammonium cations of these indenoisoquinolines increase affinity for DNA by electrostatic attraction to the negatively charged phosphodiester linkages of DNA prior to intercalation as has been established with polyamine derivatives related to spermine and spermidine.[25-28] Another possibility is that the aminoalkyl derivatives of the indenoisoquinolines could be actively transported into cells similarly to the polyamines.[25-31]

Several cases allow the comparison of substituted and unsubstituted indenoisoquinolines having the same substituents on the lactam nitrogen. For example, comparison of the unsubstituted 2-aminoethyl compound **9** (MGM 0.53, top 1 +++) with the substituted

compound **39** (MGM 0.34 μM, top1 ++++)[11] documents a relatively small contribution of the methylenedioxy and di(methoxy) substituents to the biological activity in this case. A similar trend can be observed in the comparison of the unsubstituted compound **13** (MGM 0.32 μM, top1 +++) with the substituted compound **41** (MGM 0.16 μM, top1 +++).[9] Likewise, the unsubstituted indenoisoquinoline **16** (MGM 1.86 μM, top1 +++), having a 3-dimethylaminopropyl substituent on the lactam nitrogen, is less active than the corresponding substituted compound **42** (MGM 0.35 μM, top1 ++++).[11] In all of these cases, a similar trend is observed indicating a small, but discernible and consistent contribution of the two methoxy and methylenedioxy groups to the cytotoxicity.

Given the trend toward small increases in cytotoxicity with greater substitution on the two aromatic rings, it was of interest to see how compound **35**, having an intermediate level of substitution, would fare in the cytotoxicity assay. Interestingly, the MGM of **35** (0.25 μM) is intermediate between the unsubstituted compound **13** (MGM 0.35 μM) and the fully substituted compound **41** (MGM 0.16 μM).[9] Although the differences are very small, the same general trend is observed in this case as well. It is also interesting that the *N*-ethyl compound **31** (MGM 51.3 μM), having an intermediate level of substitution, is less active than the fully substituted *N*-ethyl compound **43** (MGM 2.4 μM).[8]

The availability of the 2-aminoethyl-substituted unsubstituted indenoisoquinoline **9** (MGM 0.53 μM, top1 +++) and its higher homologues **13** (MGM 0.32 μM, top1 +++) and **22** (MGM 0.16 μM, top1 +++) make an examination of the effect of lengthening the aminoalkyl side chain straightforward. The trend toward a slight increase in cytotoxicity as the length of the aminoalkyl side chain is lengthened is apparent.

The primary amino group at the end of the aminoalkyl chain attached to the lactam nitrogen seems to confer the highest cytotoxic activity. Conversion of the primary amino group of **13** (MGM 0.32 μM, top1 +++) to the dimethylamino group present in **16** (MGM 1.86 μM, top1 +++) resulted in a decrease in cytotoxicity that is in the same direction as that observed in going from the 3-aminopropyl compound **41**[9] (MGM 0.16 μM) to the corresponding dimethylamino analogue **42** (MGM 0.35 μM). Likewise, the incorporation of the amino group of **13** into an imidazole system (**17**, MGM 1.86 μM, top1 +++++) or a guanidine system (**15**, MGM 9.77 μM, top1 ++++) resulted in a decrease in cytotoxicity, even though both of those modifications increased the top1 inhibitory potency. The lack of correlation between the cytotoxicity and top1 inhibitory activity of the derivatives tested (Table 1) suggests a different mechanism of action than top1 inhibition in some of the cases. A similar finding was reported previously with anthracene and acridine polyamine conjugates and topoisomerase II inhibition.[32] Overall, the results demonstrate that there is not an exact correlation between cytotoxicity in cancer cell cultures and top1 inhibitory activity. Differences in cellular uptake, distribution within the cell, and additional targets within the cell may all play a role, thus making the correlation of cytotoxicity with top1 inhibitory activity less than perfect. To investigate the possibility of additional biological targets in more detail, the cytotoxicities of several indenoisoquinolines were investigated in top1-deficient P388/CPT45 cells.[33] The four compounds tested (**11**, **13**, **35**, and **42**) did show antiproliferative activity in the top1-deficient P388/CPT45 cells, implicating the existence of additional mechanisms for cell growth inhibition besides top1 targeting. However, the cells were partially resistant to compounds **11** and **13**, indicating that top1 contributes at least in part to the antiproliferative activity, while compound **42** was associated with considerable resistance, indicating that top1 is likely to be the main target. The top1-deficient cells were not resistant to indenoisoquinoline **35**, which is consistent with the potent cytotoxicity observed for this compound in the presence of relatively weak top1-inhibitory activity (Table 1).

All of the compounds were examined for induction of DNA cleavage in the 3′-end-labeled *Pvu*II/*Hind*III fragment of pBluescript SK(−) phagemid DNA in the presence of top1.[2] The resulting cleavage patterns of some of the most potent indenoisoquinolines are displayed in Figure 1. The results were compared with camptothecin (**2**) and the lead compound **1** (NSC 314622). Some, but not all, of the DNA cleavage sites observed with the indenoisoquinolines were different from each other, and there were also some differences relative to camptothecin. For example, the camptothecin band at site 37 was not seen with the indenoisoquinolines in Figure 1, and the band at site 44 was observed with the indenoisoquinolines but not with camptothecin. Also, the bands observed for cleavage at identical sites varied in intensity among the indenoisoquinolines, as well as in comparison with camptothecin. These differences are important because they indicate that different cancer cell genes could be targeted more selectively with one indenoisoquinoline vs another indenoisoquinoline. Also, similar to the situation with other anticancer drugs that share a single target (e.g. top2 and tubulin inhibitors), it can be expected that different top1 inhibitors will have different spectra of antitumor activity.[34] Similar conclusions have been reached in prior top1-DNA cleavage studies involving other indenoisoquinolines.[8,9,35,36] Finally, some of the cleavage bands were more intense at intermediate drug concentrations, but became more faint at higher concentrations. For example, very little cleavage was seen at the highest concentrations of the indenoisoquinoline **35**, even though the bands at lower concentrations were relatively intense. This could be due to inhibition of the cleavage activity of the enzyme at higher drug concentrations, or alternatively, to intercalation of the drug into DNA at higher concentrations, unwinding the DNA and thereby making it a poorer substrate for the DNA-cleaving activity of the enzyme.

As mentioned above, prior molecular modeling of the ternary complexes formed between various di(methoxy)- and methylenedioxy-substituted indenoisoquinolines, DNA, and top1 has not revealed any critical role of these indenoisoquinoline substituents that would necessarily detract from the binding of the presently reported indenoisoquinolines lacking these substituents.[10,11] To investigate this question in more detail, a molecular model has been constructed of the binding of the most potent of the presently reported unsubstituted indeno-

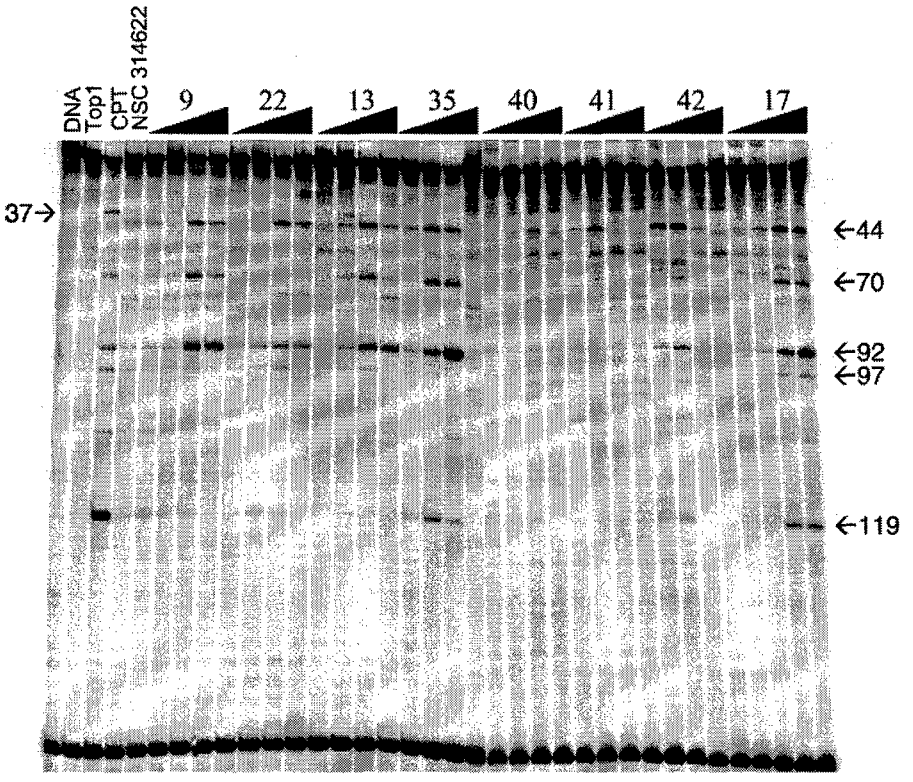

Figure 1. Comparison of the top1-mediated DNA cleavages at different drug concentrations. The DNA used corresponds to the 3′-end-labeled PvuII/HindIII fragment of pBluescript SK (−) phagemid DNA. The four concentrations of the inhibitors used were 0.1, 1.0, 10, and 100 μM. Reactions were performed at room temperature for 30 min and stopped by adding 0.5% SDS. DNA fragments were separated on 16% polyacrylamide gels. Top1 was present in all reaction mixtures except in the control lane. Control: DNA with neither top1 nor any drug. The figure is comprised of two gels, one for compounds **9**, **22**, **13**, and **35**, and another one for **40**, **41**, **42**, and **17**, that are placed side by side to facilitate comparison.

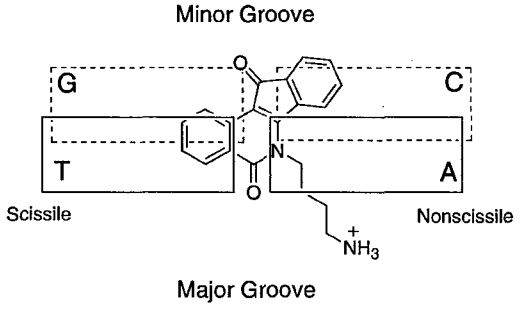

Figure 2. Hypothetical model of the orientation of indenoisoquinoline **22** relative to DNA in the ternary complex containing top1, DNA, and the inhibitor **22**.

isoquinolines, the primary amine **22**, in ternary complex with DNA and top1. To create the model, the first important decision to be made is how to orient the indenoisoquinoline with respect to the DNA. If one makes the assumption that the lactam moiety of the indenoisoquinoline **22** is oriented in the ternary complex similarly to the lactam of the clinically useful camptothecin derivative topotecan (**3**),[4] then the orientation of **22** with respect to DNA would project the aminobutyl substituent out of the duplex toward the major groove, and the ketone could point toward the minor groove (Figure 2). Using this orientation, the hypothetical model shown in Figure 3 can be fashioned starting from the published coordinates of the topotecan ternary complex.[4] To build the model, the structure of **22** was first overlapped with that of topotecan (**2**) with the lactam rings superimposed. The structure of topotecan (**2**) was then deleted, and the energy of the new indenoisoquinoline ternary complex was minimized with Sybyl, employing the MMFF94s force field and MMFF94 charges. During energy minimization, the structures of DNA, the protein, and the surrounding water molecules were frozen, and the indenoisoquinoline **22** was allowed to move. As shown in Figure 3, the indenoisoquinoline ketone moiety of the energy-minimized structure is within hydrogen bonding distance (2.2 Å) to the closest nitrogen of the guanidine group of Arg364 in the minor groove. No other important hydrogen bonding contacts of the indenoisoquinoline with the surrounding nucleic acid or protein structure are evident. As with topotecan (**2**), it is assumed that a major stabilizing force of the inhibitor on the ternary complex is its stacking interactions with the neighboring DNA bases.[4] The aminobutyl substituent is hydrogen bonded to several of the surrounding water molecules, but does not bind to the nucleic acid or protein structure. It is clear from the model that the indenoisoquinoline is capable of replacing a base pair in the DNA duplex at the cleavage site, thereby lengthening the distance between the guanine and the phosphotyrosylthymine residues and thus inhibiting the religation reaction. This would be very similar to the mechanism established for topotecan.[4]

In conclusion, a new series of indenoisoquinolines lacking aromatic substituents has been synthesized in order to probe the importance of the di(methoxy) and methylenedioxy substituents in the prior series of compounds. The results indicate that these substituents are not absolutely necessary for potent cancer cell

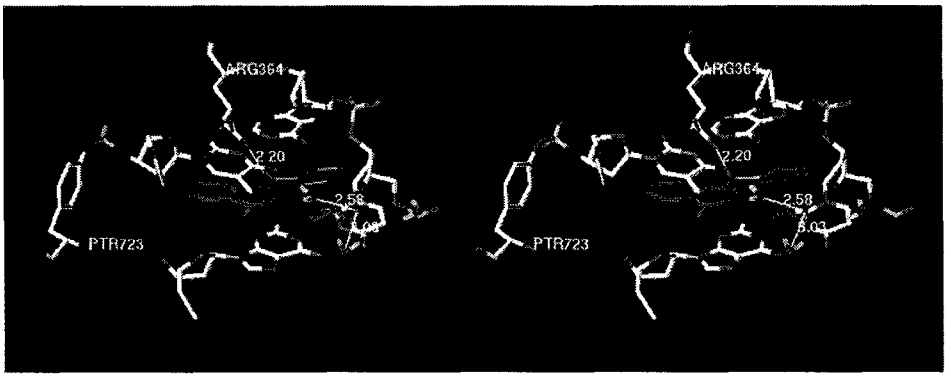

Figure 3. Hypothetical model of the binding of the indenoisoquinoline **22** in the ternary complex consisting of DNA, top1, and the inhibitor. The diagram is programmed for wall-eyed viewing.

cytotoxicity and top1 inhibitory activity, but they do consistently make a small contribution to the overall potency. Molecular modeling indicates that the unsubstituted indenoisoquinolines readily fit into ternary complexes consisting of the inhibitor, DNA, and top1, with the aminoalkyl group pointing out of the duplex into the major groove and the ketone hydrogen bonded with Arg364 in the minor groove. The unsubstituted indenoisoquinolines could offer the potential advantage of greater metabolic stability relative to their substituted counterparts, since they obviously would not be substrates for oxidative O-demethylation. Ongoing preclinical studies of the indenoisoquinolines are attempting to identify the best candidate for further development in the treatment of cancer in humans.

Experimental Section

Melting points were determined in capillary tubes and are uncorrected. Infrared spectra were obtained using $CHCl_3$ as the solvent unless otherwise specified. Except where noted, ^1H NMR spectra were obtained using $CDCl_3$ as solvent and TMS as internal standard. ^1H NMR spectra were determined at 300 or 500 MHz. Microanalyses were performed at the Purdue University Microanalysis Laboratory. Analytical thin-layer chromatography was carried out on Analtech silica gel GF 1000-μm glass plates. Compounds were visualized with short wavelength UV light. Silica gel flash chromatography was performed using 230−400 mesh silica gel. Benz[*d*]-indeno-[1,2-*b*]pyran-5,11-dione **7** was obtained commercially from Aldrich.

6-(2-Aminoethyl)-5,6-dihydro-5,11-dioxo-11*H*-indeno-[1,2-*c*]isoquinoline Hydrochloride (9). 2-(*tert*-BOC-amino)-ethylamine (0.366 g, 2.22 mmol) was added to a stirred solution of compound **7** (0.501 g, 2.02 mmol) in $CHCl_3$ (10 mL). The reaction mixture was stirred for 72 h. Chloroform (100 mL) was added to the reaction mixture, and the mixture was washed with distilled H_2O (3 × 25 mL) and brine (25 mL), dried over anhydrous $MgSO_4$, filtered, and concentrated under reduced pressure to give an orange-red solid. Purification via flash chromatography (silica gel, chloroform and 5% MeOH/$CHCl_3$) yielded crude 5,6-dihydro-5,11-dioxo-5-(ethyl-3′-*tert*-butoxycarbamoyl)-11*H*-indeno[1,2-c]isoquinoline (**8**), which was used in the next step. Crude intermediate **8** (82 mg, 0.21 mmol) was dissolved in chloroform (20 mL), an anhydrous solution of HCl in ether (1.5 mL, 3 mmol) was added, and the solution was stirred for 72 h. The precipitated product was filtered, washed with chloroform, and dried over P_2O_5 to yield the desired product **9** (45 mg, 65%): mp 274−278 °C. IR (KBr pellet) 3444, 2973, 2900, 1708, 1667, 1576, 1551, 1504 cm^{-1}; ^1H NMR (300 MHz, DMSO) δ 8.59 (d, J = 8.0 Hz, 1 H), 8.24 (d, J = 8.1 Hz, 1 H), 8.06 (s, 3 H), 7.87 (m, 2 H), 7.55 (m, 4 H), 4.76 (t, J = 6.2 Hz, 2 H), 3.24 (m, 2 H); CIMS *m/z* (rel intensity) 291 (MH^+, 77), 274 ($MH^+ - NH_3^+$, 100). Anal. ($C_{18}H_{15}ClN_2O_2 \cdot 0.44H_2O$) C, H, N, Cl.

5,6-Dihydro-6-(2-*N*-morpholinyl-1-ethyl)-5,11-dioxo-11*H*-indeno[1,2-*c*]isoquinoline (10). 4-(2-Aminoethyl)morpholine (0.3 mL, 2.2 mmol) was added to a stirred solution of compound **7** (0.502 g, 2.01 mmol) in $CHCl_3$ (10 mL). The reaction mixture was stirred for 72 h. Chloroform (100 mL) was added, and the mixture was washed with distilled H_2O (3 × 25 mL) and brine (25 mL), dried over anhydrous $MgSO_4$, filtered, and concentrated under reduced pressure to give an orange-red solid. Purification via precipitation from chloroform yielded the desired compound **10** (0.360 g, 49%): mp 193−196 °C. IR (film) 3407, 1689, 1660, 1577, 1550, 1504 cm^{-1}; ^1H NMR (300 MHz, $CDCl_3$) δ 8.71 (d, J = 7.78 Hz, 1 H), 8.33 (d, J = 8.1 Hz, 1 H), 7.75 (m, 3 H), 7.49 (m, 3 H), 4.70 (t, J = 7.6 Hz, 2 H), 3.72 (s, 4 H), 2.80 (s, 2 H), 2.60 (s, 4 H); CIMS *m/z* (rel intensity) 361 (MH^+, 100), 274 ($MH^+ - C_4H_8NO$, 57). Anal. Calcd. for ($C_{22}H_{20}N_2O_3 \cdot 0.125CHCl_3$) C, H, N, Cl.

5,6-Dihydro-5,11-dioxo-6-(2-*N*-piperazine-1-ethyl)-11*H*-indeno[1,2-*c*]isoquinoline (11). 1-(2-Aminoethyl)piperazine (0.3 mL, 2.2 mmol) was added to a stirred solution of compound **7** (0.495 g, 2.01 mmol) in $CHCl_3$ (10 mL). The reaction mixture stirred for 120 h. Chloroform (100 mL) was added, and the mixture was washed with distilled H_2O (3 × 25 mL) and brine (25 mL), dried over anhydrous $MgSO_4$, filtered, and concentrated under reduced pressure to give an orange-red solid. Purification via flash chromatography (silica gel, 6% MeOH/$CHCl_3$) yielded the desired compound **11** (0.084 g, 12%): mp 179−185 °C. IR (film) 3399, 1694, 1663, 1575, 1550, 1504 cm^{-1}; ^1H NMR (300 MHz, $CDCl_3$) δ 8.70 (d, J = 7.8 Hz, 1 H), 8.33 (d, J = 8.2 Hz, 1 H), 7.74 (m, 2 H), 7.63 (m, 1 H), 7.48 (m, 3 H), 4.69 (t, J = 7.6 Hz, 2 H), 2.94 (t, J = 4.7 Hz, 4 H), 2.81 (t, J = 7.9 Hz, 2 H), 2.61 (d, J = 4.3 Hz, 4 H), 1.79 (s, 1 H); CIMS *m/z* (rel intensity) 360 (MH^+, 100), 274 ($MH^+ - C_4H_9N_2$, 58). Anal. ($C_{22}H_{21}N_3O_2 \cdot 0.1CHCl_3$) C, H, N, Cl.

6-(3′-*tert*-BOC-aminopropyl)-5,6-dihydro-5,11-dioxo-11*H*-indeno[1,2-*c*]isoquinoline (12). 3-(*tert*-BOC-amino)-propylamine (0.383 g, 2.22 mmol) was added to a stirred solution of compound **7** (0.500 g, 2.01 mmol) in $CHCl_3$ (10 mL). The reaction mixture stirred for 48 h. Chloroform (100 mL) was added, and the mixture was washed with distilled H_2O (3 × 25 mL) and brine (25 mL), dried over anhydrous $MgSO_4$, filtered and concentrated under reduced pressure to give a crude orange-red solid. Purification via flash chromatography (silica gel, chloroform) yielded the desired compound **12** (0.665 g, 81%): mp 189−190 °C. IR (film) 3362, 3065, 2977, 1697, 1576, 1550, 1504 cm^{-1}; ^1H NMR (300 MHz, $CDCl_3$) δ 8.72 (d, J = 8.3 Hz, 1 H), 8.34 (d, J = 8.1 Hz, 1 H), 7.74 (t, J = 8.2 Hz, 1 H), 7.63 (d, J = 6.6 Hz, 1 H), 7.54 (d, J = 7.3 Hz, 1 H), 7.46 (m, 3 H), 5.35 (s, 1 H), 4.63 (t, J = 6.6 Hz, 2 H), 3.27 (m, 2 H), 2.07 (m, 2 H), 1.46 (s, 9 H); CIMS *m/z* (rel intensity) 405 (MH^+, 17), 305 ($MH^+ - CO_2C(CH_3)_3$, 100). Anal. ($C_{24}H_{24}N_2O_4 \cdot 0.7H_2O$) C, H, N

6-(3-Aminopropyl)-5,6-dihydro-5,11-dioxo-11*H*-indeno-[1,2-*c*]isoquinoline Hydrochloride (13). 6-(3′-*tert*-BOC-aminopropyl)-5,6-dihydro-5,11-dioxo-11*H*-indeno[1,2-c]isoquinoline (**12**) (0.077 g, 0.19 mmol) was dissolved in chloroform (20 mL), an anhydrous solution of 2.0 M HCl in diethyl ether

(1.5 mL, 3 mmol) was added, and the mixture was stirred for 72 h. The precipitated product was filtered, washed with chloroform, and dried over P_2O_5 for 72 h to yield the desired compound (0.065 g, 65%): mp 281–283 °C. IR (KBr pellet) 3444, 3136, 2969, 1711, 1634, 1591, 1570, 1548, 1504 cm^{-1}; ^1H NMR (300 MHz, DMSO) δ 8.59 (d, J = 8.1 Hz, 1 H), 8.23 (d, J = 8.2 Hz, 1 H), 7.93 (s, 3 H), 7.86 (t, J = 8.4 Hz, 2 H), 7.62 (m, 4 H), 4.59 (t, J = 8.7 Hz, 2 H), 3.00 (t, J = 7.2 Hz, 2 H), 2.15 (m, 2 H); CIMS *m/z* (rel intensity) 305 ($MH^+ - Cl^-$, 100), 288 ($MH^+ - NH_3{}^+Cl^-$, 52). Anal. ($C_{19}H_{17}ClN_2O_2 \cdot 0.3H_2O$) C, H, N

6-(3-Guanidinyl-1-propyl)-5,6-dihydro-5,11-dioxo-11*H*-indeno[1,2-*c*]isoquinoline Trifluoroacetate (15). A solution of 1,3-bis(*tert*-butoxycarbonyl)-2-methyl-2-pseudourea (0.23 g, 0.79 mmol) in dry THF (60 mL) was added dropwise to a stirred solution of amine **14** (0.12 g, 0.40 mmol) and $HgCl_2$ (10 mg) in THF–H_2O (40 mL, 20:1, v/v) at 50 °C, and the mixture was stirred for 2 h at that temperature and further stirred at room temperature for 5 h. The reaction mixture was concentrated and diluted with $CHCl_3$ (50 mL). The organic portion was washed with 10% aq $NaHCO_3$ and water, dried (Na_2SO_4), and concentrated. The organic residue was loaded on a silica gel column (60 g, 60–200 mesh) and eluted with a 19:1 gradient of $CHCl_3$–Et_3N mixture to give the 3-guanidinyl compound (0.14 g, 0.26 mmol, 65%) as an oil, which was further treated with neat CF_3COOH (20 mL) at room temperature for 2 h. The reaction mixture was concentrated and diluted with chloroform (50 mL), and the resulting solid was filtered through a sintered glass funnel, washed with chloroform (20 mL) and dichloromethane (20 mL), and dried to provide indenoisoquinoline **15** (110 mg, 62%) as a pale red solid: mp 232–234 °C. ^1H NMR (300 MHz, DMSO-d_6) δ 8.58 (d, J = 8.3 Hz, 1 H), 8.22 (d, J = 7.8 Hz, 1 H), 7.83 (t, J = 7.0 Hz, 1 H), 7.74 (d, J = 7.5 Hz, 1 H), 7.61–7.49 (m, 4 H), 7.16 (bs, 3 H, 3 × –NH-), 4.53 (bs, 2 H), 3.36 (bs, 2 H), 2.00 (m, 2 H); ESIMS *m/z* (rel intensity) 348 (22), 347 ($MH^+ - 3 \times CF_3COOH$, 100), 288 (21). Anal. ($C_{22}H_{19}F_3N_4O_4 \cdot 1.2H_2O$) C, H, N.

5,6-Dihydro-6-(3-(dimethylamino)-1-propyl)-5,11-dioxo-11*H*-indeno[1,2-*c*]isoquinoline (16). 3-(Dimethylamino)-propylamine (0.25 g, 2.4 mmol) was added to a stirred solution of compound **7** (0.5 g, 2.0 mmol) in chloroform (50 mL), and the reaction mixture was stirred at room temperature for 12 h. The precipitated product was filtered off, washed with ether–chloroform (50 mL, 2:1) and dried to obtain pure indenoisoquinoline **16** (0.47 g, 70%) as an orange solid: mp 168–171 °C. ^1H NMR (300 MHz, $CDCl_3$) δ 8.67 (d, J = 8.1 Hz, 1 H), 8.32–8.29 (dt, J = 0.7 and 8.1 Hz, 1 H), 7.75–7.67 (m, 2 H), 7.60 (dt, J = 1.0 and 6.6 Hz, 1 H), 7.46–7.33 (m, 4 H), 4.56 (t, J = 7.9 Hz, 2 H), 2.50 (t, J = 6.6 Hz, 2 H), 2.29 (s, 6 H), 2.07–1.98 (m, 2 H); ESIMS *m/z* (rel intensity) 334 (23), 333 (MH^+, 100), 289 (10), 288 (48). Anal. ($C_{21}H_{20}N_2O_2 \cdot 0.4CH_2Cl_2$) C, H, N.

5,6-Dihydro-6-(3-imidazolyl-1-propyl)-5,11-dioxo-11*H*-indeno[1,2-*c*]isoquinoline Hydrochloride (17). 1-(3-Aminopropyl)imidazole (0.23 g, 1.8 mmol) was added to a stirred solution benz[*d*]-indeno[1,2-*b*]pyran-5,11-dione **7** (0.5 g, 2.0 mmol) in chloroform (50 mL), and the reaction mixture was stirred at room temperature for 12 h. The reddish-brown precipitate was dissolved in chloroform (150 mL), and 2 M HCl in ether (10.0 mL, 20.0 mmol) was added slowly to the reaction mixture, which was stirred at room temperature for 5 h. The product was filtered off through a sintered glass funnel, washed with chloroform (50 mL), and dried to obtain pure indenoisoquinoline hydrochloride **17** (0.65 g, 82%) as a pale red solid: mp 266–268 °C. ^1H NMR (300 MHz, $CDCl_3$) δ 9.18 (s, 1 H), 8.57 (d, J = 8.1 Hz, 1 H), 8.20 (d, J = 8.1 Hz, 1 H), 7.85–7.80 (m, 2 H), 7.70–7.66 (m, 2 H), 7.60–7.48 (m, 4 H), 4.55 (t, J = 6.6 Hz, 2 H), 4.40 (t, J = 7.2 Hz, 2 H), 2.39 (m, 2 H); ESIMS *m/z* (rel intensity) 357 (23), 356 (MH^+ – HCl, 100), 289 (9), 288 (45). Anal. ($C_{22}H_{18}ClN_3O_2 \cdot 0.4H_2O$) C, H, N.

6-(3-Bromo-1-propyl)-5,11-dioxo-11*H*-indeno[1,2-*c*]isoquinoline (18) and 5,6-Dihydro-6-[(3-triethylammonium)-1-propyl]-5,11-dioxo-11*H*-indeno[1,2-*c*]isoquinoline Bromide (19). Triethylamine (0.85 mL, 6.1 mmol) was added to a stirred solution of 3-bromopropylamine hydrobromide (0.53 g, 2.4 mmol) in chloroform (100 mL), and the reaction mixture was stirred at room temperature for 30 min. Then compound **7** (0.5 g, 2.0 mmol) was added to the reaction mixture at room temperature, and the reaction mixture was stirred at the same temperature for 60 h. The crude reaction product was directly loaded on a silica gel column (60–210 mesh, 70 g) and eluted with a 0–1% gradient of methanol in chloroform to afford indenoisoquinoline bromide **18**[9] (0.32 g, 43%) and indenoisoquinoline ammonium bromide **19** (0.46 g, 49%) as orange solids. Compound **19**: mp 142–144 °C. ^1H NMR (300 MHz, $CDCl_3$) δ 8.69 (d, J = 8.3 Hz, 1 H), 8.33 (d, J = 7.5 Hz, 1 H), 7.75–7.66 (m, 2 H), 7.63–7.60 (dd, J = 1.0 and 6.7 Hz, 1 H), 7.49–7.35 (m, 3 H), 4.70 (t, J = 6.6 Hz, 2 H), 3.70 (q, J = 5.9 Hz, 2 H), 3.16–3.07 (m, 6 H), 2.16–2.08 (m, 2 H), 1.42 (t, J = 7.3 Hz, 9 H); ESIMS *m/z* (rel intensity) 389 (MH^+ – Br, 19), 364 (15), 363 (MH^+,-CH_2CH_3, 100), 347 (31). Anal. ($C_{25}H_{29}N_2O_2Br \cdot 0.2CHCl_3$) C, H, N.

5,6-Dihydro-6-[3-(3-imidazolylpropyl)amino-1-propyl]-5,11-dioxo-11*H*-indeno[1,2-*c*]isoquinoline Di(hydrochloride) (20). A mixture of indenoisoquinoline bromide **18** (0.25 g, 0.68 mmol), 1-(3-aminopropyl)imidazole (0.43 g, 3.4 mmol), and anhydrous K_2CO_3 (0.28 g, 2.0 mmol) in anhydrous 1,4-dioxane (20 mL) was heated to 100 °C and kept at that temperature for 4 h. The reaction mixture was cooled and concentrated on a rotary evaporator. The reaction mixture was diluted with chloroform (100 mL), washed with 1% HCl solution (50 mL), water, and brine, and dried (Na_2SO_4). The reaction mixture was concentrated, loaded on a silica gel column, and eluted with a 0–5% gradient of methanol in chloroform to provide indenoisoquinoline (180 mg, 0.44 mmol, 64%), which was further treated with 2 M HCl in ether (4.4 mL, 8.80 mmol) in chloroform (30 mL) at room temperature for 4 h to afford indenoisoquinoline hydrochloride **20** (170 mg, 80%) as a pale orange solid: mp 264–266 °C (dec). ^1H NMR (300 MHz, DMSO-d_6) δ 9.09 (bs, 2 H, –NH- and imidazole H), 8.59 (d, J = 8.1 Hz, 1 H), 8.23 (d, J = 9.0 Hz, 1 H), 7.83 (d, J = 7.0 Hz, 1 H), 7.76 (bs, 1 H), 7.61–7.52 (m, 5 H), 4.58 (bs, 2 H), 4.32 (bs, 2 H), 3.08 (bs, 2 H), 2.87 (bs, 2 H), 2.19 (bs, 4 H); ESIMS *m/z* (rel intensity) 414 (27), 413 ($MH^+ - 2 \times HCl$, 100), 346 (16), 345 (63), 289 (12), 288 (58). Anal. ($C_{25}H_{26}Cl_2N_4O_2 \cdot 0.5CHCl_3$) C, H, N.

6-[(4-*tert*-BOC-amino)-5,6-dihydro-1-butyl]-5,11-dioxo-11*H*-indeno[1,2-*c*]isoquinoline (21). 4-(*tert*-BOC-amino)-butylamine (0.5 g, 2.7 mmol) was added to a stirred solution of compound **7** (0.6 g, 2.4 mmol) in chloroform (50 mL), and the reaction mixture was stirred at room temperature for 12 h. The reaction product was directly loaded on a silica gel column (60–210 mesh, 70 g) and eluted with a 0–1% gradient of methanol in chloroform to afford indenoisoquinoline **21** (0.91 g, 78%) as a orange solid: mp 158–160 °C. ^1H NMR (300 MHz, $CDCl_3$) δ 8.67 (d, J = 8.1 Hz, 1 H), 8.30 (d, J = 8.0 Hz, 1 H), 7.70 (t, J = 7.3 Hz, 1 H), 7.60 (d, J = 6.2 Hz, 1 H), 7.44–7.34 (m, 4 H), 4.66 (bs, 1 H, –NH), 4.51 (t, J = 7.3 Hz, 2 H), 3.21 (m, 2 H), 1.92–1.87 (m, 2 H), 1.73–1.68 (m, 2 H), 1.41 (s, 9 H); ESIMS *m/z* (rel intensity) 442 (23), 441 (MNa^+, 100), 419 (MH^+, 24), 320 (11), 319 (MH^+ – Boc, 56), 311 (48), 302 (28). Anal. ($C_{25}H_{26}N_2O_4$) C, H, N.

6-(4-Amino-1-butyl)-5,6-dihydro-5,11-dioxo-11*H*-indeno-[1,2-*c*]isoquinoline Hydrochloride (22). Boc-protected indenoisoquinoline **21** (0.5 g, 1.2 mmol) was dissolved in chloroform (50 mL), and an anhydrous solution of 2.0 M HCl in ether (2 M, 11.5 mL, 23.0 mmol) was added. The reaction mixture was stirred at room temperature for 5 h. The precipitated product was filtered off, washed with chloroform (50 mL), and dried over P_2O_5 for 24 h to afford pure indenoisoquinoline hydrochloride **22** (0.38 g, 88%) as a red solid: mp 268–270 °C. ^1H NMR (300 MHz, DMSO-d_6) δ 8.55 (d, J = 8.0 Hz, 1 H), 8.20 (d, J = 8.3 Hz, 1 H), 7.93 (bs, 2 H, $-NH_2$), 7.81 (t, J = 7.6 Hz, 1 H), 7.72 (d, J = 7.3 Hz, 1 H), 7.61–7.47 (m, 4 H), 4.51 (bs, 2 H), 2.82 (bs, 2 H), 1.85 (bs, 2 H), 1.72 (m, 2 H); ESIMS *m/z* (rel intensity) 320 (22), 319 (MH^+ – HCl, 100). Anal. ($C_{20}H_{19}N_2O_2Cl \cdot 0.5H_2O$) C, H, N.

***cis*-4-Carboxy-*N*-ethyl-3,4-dihydro-3-(3,4-methylenedioxyphenyl)-1-(2*H*)-isoquinolone (28).** Imine **24**[8] (2.73 g, 15.4 mmol) was placed in a 100 mL round-bottomed flask and dissolved in $CHCl_3$ (25 mL). The solution was cooled in an ice bath to 0 °C. Homophthalic anhydride **(27)** (2.50 g, 15.4 mmol) was added to the mixture over 1 h in portions every 20 min. The mixture was then allowed to return to room temperature while being stirred for 12 h. The solid was filtered off and purified by precipitation from $CHCl_3$, producing **28** as a white solid (0.273 g, 5%): mp 178–180 °C. IR (film) 2979, 1735, 1627, 1490, 1253, 1039 cm^{-1}; ^1H NMR (300 MHz, DMSO-d_6) δ 7.99 (d, J = 6.6 Hz, 1 H), 7.55 (d, J = 7.5 Hz, 1 H), 7.50 (dt, J = 1.5 and 7.5 Hz, 1 H), 7.42 (t, J = 6.9 Hz, 1 H), 6.74 (d, J = 8.1 Hz, 1 H), 6.53 (dd, J = 1.5 and 7.8 Hz, 1 H), 6.43 (d, J = 1.5 Hz, 1 H), 5.92 (s, 2 H), 5.06 (d, J = 6.3 Hz, 1 H), 4.63 (d, J = 6.3 Hz, 1 H), 3.76 (m, 1 H), 3.00 (m, 1 H), 1.03 (t, J = 7.0 Hz, 3 H); ESIMS *m/z* (rel intensity) 340 (MH^+, 100). Anal. ($C_{19}H_{17}NO_5 \cdot 0.13CHCl_3$) C, H, N.

***cis*-4-Carboxy-*N*-propyl-3,4-dihydro-3-(3,4-methylenedioxyphenyl)-1-(2,*H*)-isoquinolone (29).** Imine **25**[37] (2.88 g, 15.1 mmol) was placed in a 250 mL round-bottomed flask and dissolved in $CHCl_3$ (75 mL). Homophthalic anhydride **(27)** (2.44 g, 15.1 mmol) was added to the mixture in one portion. The mixture was then stirred at room temperature for 16 h and concentrated to ~35 mL and the product precipitated upon addition of hexanes (20 mL). The solid was filtered off and washed with hexanes (50 mL) and diethyl ether (50 mL), producing **29** as an off-white solid (2.65 g, 50%): mp 175–177 °C. IR (film) 2966, 1743, 1621, 1598, 1572, 1505, 1489, 1445, 1252, 1039, and 749 cm^{-1}; ^1H NMR (300 MHz, DMSO-d_6) δ 8.25 (dd, J = 6.6 and 1.7 Hz, 1 H), 7.53–1.45 (m, 3 H), 6.63 (d, J = 8.0 Hz, 1 H), 6.56 (dd, J = 8.0 and 1.83 Hz, 1 H), 6.44 (d, J = 1.7 Hz, 1 H), 5.89 (dd, J = 5.1 and 1.4 Hz, 2 H), 4.96 (d, J = 6.3 Hz, 1 H), 4.73 (d, J = 6.3 Hz, 1 H), 4.01–3.93 (m, 1 H), 2.90–2.82 (m, 1 H), 1.71–1.61 (m, 2 H), 0.97 (t, J = 7.3 Hz, 3 H); CIMS *m/z* (rel intensity) 354 (MH^+, 100). Anal. ($C_{20}H_{19}NO_5 \cdot 0.11CHCl_3$) C, H, N

***cis*-*N*-(3-Bromopropyl)-4-carboxy-3,4-dihydro-3-(3,4-methylenedioxyphenyl)-1(2*H*)-isoquinolone (30).** Imine **26**[38] (2.50 g, 9.26 mmol) was added to a 100 mL round-bottomed flask along with $CHCl_3$ (75 mL). The solution was cooled in an ice bath to 0 °C. Homophthalic anhydride **(27)** (2.00 g, 9.26 mmol) was added to the mixture over 1 h in portions every 20 min. The mixture was then allowed to return to room temperature while being stirred for 12 h. The precipitate was collected by vacuum filtration before washing the solid four times with $CHCl_3$, leaving a white solid (0.653 g, 16%): mp 177–180 °C. IR (neat) 2939, 1746, 1615, 1597, 1571, 1489, 1503, 1446, 1258, and 1040 cm^{-1}; ^1H NMR (500 MHz, DMSO-d_6) δ 12.98 (bs, 1 H), 7.95 (d, J = 7.5 Hz, 1 H), 7.48 (m, 2 H), 7.38 (t, J = 17.0 Hz, 1 H), 6.71 (d, J = 8.1 Hz, 1 H), 6.46 (dd, J = 1.4 and 8.03 Hz, 1 H), 6.35 (d, J = 1.4 Hz, 1 H), 5.88 (s, 2 H), 5.00 (d, J = 6.2 Hz, 1 H), 4.75 (d, J = 5.9 Hz, 1 H), 3.82 (m, 1 H), 3.48 (m, 1 H), 2.90 (m, 1 H), 2.08 (m, 1 H), 1.96 (m, 1 H); ESIMS *m/z* (rel intensity) 352 (100 MH^+ – HBr). Anal. ($C_{20}H_{18}BrNO_5 \cdot 0.8H_2O$) C, H, N.

6-(3-Ethyl)-5,6-dihydro-8,9-methylenedioxy-5,11-dioxo-11*H*–indeno[1,2-*c*]isoquinoline (31). Imine **24**[8] (2.73 g, 0.015 mol) was placed in a 250 mL round-bottomed flask before dissolving it in $CHCl_3$ (100 mL). The solution was cooled in an ice bath to 0 °C. Next, homophthalic anhydride **(27)** (2.50 g, 0.0154 mol) was added to the mixture over 1 h in portions every 20 min. The mixture was then allowed to return to room temperature while being stirred for 12 h. The mixture was concentrated in vacuo to produce a viscous yellow oil, suggesting a mixture of cis and trans acids. The cis acid was unable to be separated, and therefore the crude yellow oil was placed into the next reaction. Subsequently, the oil was dissolved in $SOCl_2$ (100 mL) before stirring for 4 h. Next, the solution was concentrated in vacuo before redissolving in toluene three times (3 × 100 mL). After each dissolution, the solution was concentrated in vacuo to form a solid. The liquid was purified by flash chromatography (silica gel, $CHCl_3$) to provide a solid. This solid was further purified by precipitation from $CHCl_3$. The mixture was cooled for 12 h before filtering the solid (0.325 g, 7.0%) out of the solvent: mp 263–265 °C. IR (film) 1660, 1504, 1429, 1309, 1270, and 788 cm^{-1}; ^1H NMR (300 MHz, $CDCl_3$) δ 8.60 (d, J = 8.1 Hz, 1 H), 8.30 (d, J = 7.8 Hz, 1 H), 7.69–7,63 (m, 1 H), 7.41–7.37 (m, 1 H), 7.11 (s, 1 H), 7.04 (s, 1 H), 6.09 (s, 2 H), 4.54 (q, J = 7.2 Hz, 2 H), 1.51 (t, J = 7.2 Hz, 3 H); CIMS *m/z* (rel intensity) 414 (100, MH^+). Anal. ($C_{19}H_{13}NO_4 \cdot 0.3H_2O$) C, H, N.

5,6-Dihydro-8,9-methylenedioxy-5,11-dioxo-6-propyl-11*H*-indeno[1,2-*c*]isoquinoline (32). Imine **25**[35] (3.32 g, 17.4 mmol) was placed in a 250 mL round-bottomed flask and dissolved in $CHCl_3$ (125 mL). The solution was cooled in an ice bath to 0 °C. Homophthalic anhydride **(27)** (2.815 g, 17.4 mmol) was added to the mixture over 1 h in portions every 20 min. The mixture was then allowed to return to room temperature while being stirred for 12 h. The mixture was concentrated in vacuo to produce a viscous yellow oil, and NMR analysis suggested a mixture of cis acid **29** and the corresponding trans acid. The oil was dissolved in $SOCl_2$ (100 mL) and the mixture stirred for 4 h. The solution was concentrated in vacuo before dissolving it in toluene (3 × 100 mL). The mixture was concentrated, dissolved in toluene (100 mL), and concentrated to yield a solid that was removed by filtration. This procedure was repeated twice, resulting in removal of additional solid. The remaining liquid was purified by flash chromatography (silica gel, $CHCl_3$) to provide a solid, which was precipitated from $CHCl_3$ to provide the product as a solid (0.234 g, 4%): mp 229–230 °C. IR (film) 1662, 1500, 1427, 1310, and 751 cm^{-1}; ^1H NMR (300 MHz, $CDCl_3$) δ 8.59 (d, J = 8.1 Hz, 1 H), 8.28 (d, J = 7.5 Hz, 1 H), 7.66 (dt, J = 1.5 and 7.8 Hz, 1 H), 7.39 (dt, J = 1.2 and 7.5 Hz, 1 H), 7.11 (s, 1 H), 6.94 (s, 1 H), 6.09 (s, 2 H), 4.38 (t, J = 8.1 Hz, 2 H), 1.90 (m, 2 H), 1.11 (t, J = 7.5 Hz, 3 H); EIMS *m/z* (rel intensity) 333 (M^+, 57), 291 ($M^+ - C_3H_6$, 100). Anal.($C_{20}H_{15}NO_4 \cdot 0.4H_2O$) C, H, N.

6-(3-Bromopropyl)-5,6-dihydro-8,9-methylenedioxy-5,11-dioxo-11*H*-indeno[1,2-*c*]isoquinoline (33). Cis acid **30** (2.890 g, 6.690 mmol) was added to a 250 mL round-bottomed flask along with $SOCl_2$ (160 mL). The solution was capped with a glass stopper and stirred for 4 h. The solution was concentrated in vacuo to form a solid. The compound was purified by flash chromatography (silica gel, $CHCl_3$) to provide a purple solid. This product was further purified by precipitation from $CHCl_3$, yielding a solid (0.288 g, 10%): mp 214–216 °C. IR (neat) 1657, 1610, 1502, 1483, 1426, 1376 1297, 1035, and 786 cm^{-1}; ^1H NMR (300 MHz, $CDCl_3$) δ 8.59 (d, J = 8.1 Hz, 1 H), 8.27 (d, J = 7.2 Hz, 1 H), 7.68 (dt, J = 1.5 and 8.4 Hz, 1 H), 7.40 (dt, J = 1.2 and 8.1 Hz, 1 H), 7.34 (s, 1 H), 7.12 (s, 1 H), 6.09 (s, 2 H), 4.59 (t, J = 7.8 Hz, 2 H), 3.63 (t, J = 6.3 Hz, 2 H), 2.44 (m, 2 H); CIMS *m/z* (rel intensity) 414 (100, MH^+). Anal. ($C_{20}H_{14}BrNO_4 \cdot 0.2H_2O$) C, H, N.

6-(3-Azidopropyl)-5,6-dihydro-8,9-methylenedioxy-5,11-dioxo-11*H*-indeno[1,2-*c*]isoquinoline (34). A solution of **33** (0.090 g, 0.218 mmol) and NaN_3 (0.043 g, 0.66 mmol) in DMSO (10 mL) was stirred at room temperature for 26 h. The solution was diluted with $CHCl_3$ (100 mL) and washed with H_2O (3 × 25 mL) and sat. NaCl (25 mL). The organic layer was dried over sodium sulfate, filtered, and concentrated to provide a red-brown solid (0.079 g, 96%): mp 197 °C (dec). IR (film) 2092, 1655, 1546, 1508, 1478, 1425, 1296, and 1037 cm^{-1}; ^1H NMR (300 MHz, DMSO-d_6) δ 8.49 (d, J = 8.0 Hz, 1 H), 8.19 (d, J = 8.0 Hz, 1 H), 7.80 (t, J = 7.6 Hz, 1 H), 7.49 (m, 2 H), 7.17 (s, 1 H), 6.22 (s, 2 H), 4.52 (t, J = 7.7 Hz, 2 H), 3.63 (t, J = 6.5 Hz, 2 H), 2.03 (m, 2 H); CIMS *m/z* (rel intensity) 375 (100, MH^+). Anal. Calcd for ($C_{20}H_{14}N_4O_4 \cdot 0.05CHCl_3$) C, H, N

6-(3-Aminopropyl)-5,6-dihydro-8,9-methylenedioxy-5,11-dioxo-11*H*-indeno[1,2-*c*]isoquinoline Hydrochloride Salt (35). A 50 mL flame-dried flask was charged with **34** (0.100 g, 0.268 mmol), anhydrous benzene (25 mL), and triethyl phosphite (0.114 mL, 0.665 mmol), and the solution was heated at reflux for 16 h. The solution was cooled to room temperature, and 3 N HCl in methanol (10 mL) was added. The solution was heated at reflux for 2 h. The solution was cooled to room temperature, followed by additional chilling at

0 °C for 1 h. The precipitate was filtered and washed with cold methanol (2 mL) to provide a red solid (0.087 g, 84%): mp 277 °C (dec); IR (film) 2910, 1549, 1483, 1428, 1378, 1302, 1034, and 785 cm^{-1}; ^1H NMR (300 MHz, DMSO-d_6) δ 8.47 (d, J = 8.0 Hz, 1 H), 8.16 (d, J = 7.8 Hz, 1 H), 7.86 (bs, 2 H), 7.78 (t, J = 7.3 Hz, 1 H), 7.47 (m, 1 H), 6.22 (s, 2 H), 4.51 (t, J = 6.7 Hz, 2 H), 2.94 (bs, 2 H), 2.09 (t, J = 7.4 Hz, 2 H); ESIMS *m/z* (rel intensity) 349 (MH^+ − Cl, 100). Anal. ($C_{20}H_{17}ClN_2O_4 \cdot 1.0H_2O$) C, H, N.

Top1-Mediated DNA Cleavage Reactions. Human recombinant top1 was purified from Baculovirus as described previously.[12] The 161 bp fragment from pBluescript SK(−) phagemid DNA (Stratagene, La Jolla, CA) was cleaved with the restriction endonuclease *Pvu*II and *Hin*dIII (New England Biolabs, Beverly, MA) in supplied NE buffer 2 (50 μL reactions) for 1 h at 37 °C and separated by electrophoresis in a 1% agarose gel made in 1X TBE buffer. The 161 bp fragment was eluted from the gel slice using the QIAEX II kit (QIAGEN Inc., Valencia, CA). Approximately 200 ng of the fragment was 3′-end labeled at the *Hin*dIII site by fill-in reaction with [alpha-^{32}P]-dGTP and 0.5 mM dATP, dCTP, and dTTP, in React 2 buffer (50 mM Tris-HCl, pH 8.0, 100 mM $MgCl_2$, 50 mM NaCl) with 0.5 units of DNA polymerase I (Klenow fragment). Unincorporated ^{32}P-dGTP was removed using mini Quick Spin DNA columns (Roche, Indianapolis, IN), and the eluate containing the 3′-end-labeled 161 bp fragment was collected. Aliquots (approximately 50 000 dpm/reaction) were incubated with top1 at 22 °C for 30 min in the presence of the tested drug. Reactions were terminated by adding SDS (0.5% final concentration).[2] The samples (10 μL) were mixed with 30 μL of loading buffer (80% formamide, 10 mM sodium hydroxide, 1 mM sodium EDTA, 0.1% xylene cyanol, and 0.1% bromophenol blue, pH 8.0). Aliquots were separated in denaturing gels (16% polyacrylamide, 7 M urea). Gels were dried and visualized by using a Phosphoimager and ImageQuant software (Molecular Dynamics, Sunnyvale, CA).

Molecular Modeling. The structure of the ternary complex, containing topoisomerase I, DNA, and topotecan, was downloaded from the Protein Data Bank (PDB code 1K4T).[4] One molecule of PEG and the topotecan carboxylate form were deleted. All of the atoms were then fixed according to Sybyl atom types. Hydrogens were added and minimized using the MMFF94s force field and MMFF94 charges. The structure of the indenoisoquinoline **2**, constructed in Sybyl and energy minimized with the Tripos force field and Gasteiger-Hückel charges, was overlapped with the structure of topotecan according to the proposed structural similarity[10] in the ternary complex, and the structure of topotecan was then deleted. The new whole complex was subsequently subjected to energy minimization using the MMFF94s force field with MMFF94 charges. During energy minimization, the structure of the indenoisoquinoline was allowed to move while the structures of the protein, nucleic acid, and water molecules were frozen. The energy minimization was performed using the Powell method with a 0.05 kcal/mol·Å energy gradient convergence criterion and a distance-dependent dielectric constant.

Acknowledgment. Part of this work was supported with Research Grant UO1 CA89566 and Training Grant ST32 CA09634-12. The in vitro and in vivo testing was conducted through the Developmental Therapeutics Program, DCTD, NCI under Contract NO1-CO-56000.

Supporting Information Available: Elemental analyses. This material is available free of charge via the Internet at http://pubs.acs.org.

References

(1) Cushman, M.; Cheng, L. Stereoselective Oxidation by Thionyl Chloride Leading to the Indeno[1,2-c]isoquinoline System. *J. Org. Chem.* **1978**, *43*, 3781−3783.

(2) Kohlhagen, G.; Paull, K.; Cushman, M.; Nagafuji, P.; Pommier, Y. Protein-Linked DNA Strand Breaks Induced by NSC 314622, a Novel Noncamptothecin Topoisomerase I Poison. *Mol. Pharmacol.* **1998**, *54*, 50−58.

(3) Pommier, Y.; Pourquier, P.; Fan, Y.; Strumberg, D. Mechanism of Action of Eukaryotic DNA Topoisomerases and Drugs Targeted to the Enzyme. *Biochim. Biophys. Acta* **1998**, *1400*, 83−105.

(4) Staker, B. L.; Hjerrild, K.; Feese, M. D.; Behnke, C. A.; Burgin Jr., A. B.; Stewart, L. The Mechanism of Topoisomerase I Poisoning by a Camptothecin Analogue. *Proc. Natl. Acad. Sci. U.S.A.* **2002**, *99*, 15387−15392.

(5) Meng, L. H.; Liao, Z. Y.; Pommier, Y. Non-Camptothecin DNA Topoisomerase I Inhibitors in Cancer Therapy. *Curr. Topics Med. Chem.* **2003**, *3*, 305−320.

(6) Pommier, Y. Eukaryotic DNA Topoisomerase I: Genome Gate Keeper and Its Intruders, Camptothecins. *Semin. Oncol.* **1996**, *23*, 1−10.

(7) (a) Jaxel, C.; Kohn, K. W.; Wani, M. C.; Pommier, Y. Structure−Activity Study of the Actions of Camptothecin Derivatives on Mammalian Topoisomerase I: Evidence for a Specific Receptor Site and a Relation to Antitumor Activity. *Cancer Res.* **1989**, *49*, 1465−1469. (b) Minami, H.; Beijnen, J. H.; Verweij, J.; Ratain, M. J. Limited Sampling Model for Area under the Concentration Time Curve of Total Topotecan. *Clin. Cancer Res.* **1996**, *2*, 43−46. (c) Danks, M. K.; Pawlik, C. A.; Whipple, D. O.; Wolverton, J. S. Intermittent Exposure of Medulloblastoma Cells to Topotecan Produces Growth Inhibition Equivalent to Continuous Exposure. *Curr. Topics Med. Chem.* **1997**, *3*, 1731−1738. (d) Haas, N. B.; LaCreta, F. P.; Walczak, J.; Hudes, G. R.; Brennan, J. M.; Ozols, R. F.; O'Dwyer, P. J. PhaseI/Pharmacokinetic Study of Topotecan by 24-Hour Continuous Infusion Weekly. *Cancer Res.* **1994**, *54*, 1220−1226.

(8) Strumberg, D.; Pommier, Y.; Paull, K.; Jayaraman, M.; Nagafuji, P.; Cushman, M. Synthesis of Cytotoxic Indenoisoquinoline Topoisomerase I Poisons. *J. Med. Chem.* **1999**, *42*, 446−457.

(9) Cushman, M.; Jayaraman, M.; Vroman, J. A.; Fukunaga, A. K.; Fox, B. M.; Kohlhagen, G.; Strumberg, D.; Pommier, Y. Synthesis of New Indeno[1,2-c]isoquinolines: Cytotoxic Non-Camptothecin Topoisomerase I Inhibitors. *J. Med. Chem.* **2000**, *43*, 3688−3698.

(10) Fox, B. M.; Xiao, X.; Antony, S.; Kohlhagen, G.; Pommier, Y.; Staker, B. L.; Stewart, L.; Cushman, M. Design, Synthesis, and Biological Evaluation of Cytotoxic 11-Alkenylindenoisoquinoline Topoisomerase I Inhibitors and Indenoisoquinoline-Camptothecin Hybrids. *J. Med. Chem.* **2003**, *46*, 3275−3282.

(11) Nagarajan, M.; Xiao, X.; Antony, S.; Kohlhagen, G.; Pommier, Y.; Cushman, M. Design, Synthesis, and Biological Evaluation of Indenoisoquinoline Topoisomerase I Inhibitors Featuring Polyamine Side Chains on the Lactam Nitrogen. *J. Med. Chem.* **2003**, *46*, 5712−5724.

(12) Pourquier, P.; Ueng, L.-M.; Fertala, J.; Wang, D.; Park, H.-J.; Essigmann, J. M.; Bjornsti, M.-A.; Pommier, Y. Induction of Reversible Complexes between Eukaryotic DNA Topoisomerase I and DNA-containing Oxidative Base Damages. 7,8-Dihydro-8-Oxoguanine and 5-Hydroxycytosine. *J. Biol. Chem.* **1999**, *274*, 8516−8523.

(13) Antony, S.; Jayaraman, M.; Laco, G.; Kohlhagen, G.; Kohn, K. W.; Cushman, M.; Pommier, Y. Differential Induction of Topoisomerase I-DNA Cleavage Complexes by the Indenoisoquinoline MJ-III-65 (NSC 706744) and Camptothecin: Base Sequence Analysis and Activity against Camptothecin-Resistant Topoisomerase I. *Cancer Res.* **2003**, *63*, 7428−7435.

(14) Klucar, J.; Al-Rubeai, M. G2 Cell Cycle Arrest and Apoptosis Are Induced in Burkitt's Lymphoma Cells by the Anticancer Agent Oracin. *FEBS Lett.* **1997**, *400*, 127−130.

(15) Michalský, J. 6-[X-(2-Hydroxyethyl)aminoalkyl]-5, 11-dioxo-5,6-dihydro-11-H-indeno[1,2-c]isoquinolines and Their Use as Antineoplastic Agents.; VUFB a.s., Praha, Czechoslovakia: United States Patent 5,597,831, 1997.

(16) Gersl, V.; Mazurová, Y.; Bajgar, J.; Mélka, M.; Hrdina, R.; Palicka, V. Lack of Cardiotoxicity of a New Antineoplastic Agent, a Synthetic Derivative of Indenoisoquinoline: Comparison with Daunorubicin in Rabbits. *Arch. Toxicol.* **1996**, *70*, 645−651.

(17) Wsól, V.; Kvasnicková, E.; Szotáková, B.; Hais, I. M. High-performance Liquid Chromatography Assay for the Separation and Characterization of Metabolites of the Potential Cytostatic Drug Oracine. *J. Chromatogr. B* **1996**, *681*, 169−175.

(18) Marhan, J. Mutagenicity of Cytostatic Drugs in Bacterial System. I. Ames Test. *Folia Microbiol.* **1995**, *40*, 457−461.

(19) Marhan, J. Mutagenicity of Cytostatic Drugs in a Bacterial System. II. DNA-Repair Test. *Folia Microbiol.* **1995**, *40*, 462−466.

(20) Cushman, M.; Gentry, J.; Dekow, F. W. Condensation of Imines with Homophthalic Anhydrides. A Convergent Synthesis of *cis*- and *trans*-13-Methyltetrahydroprotoberberines. *J. Org. Chem.* **1977**, *42*, 1111−1116.

(21) Cushman, M.; Cheng, L. Total Synthesis of Nitidine Chloride. *J. Org. Chem.* **1978**, *43*, 286−288.

(22) Johnson, F. Steric Interference in Allylic and Pseudoallylic Systems. I. Two Stereochemical Theorems. *J. Am. Chem. Soc.* **1965**, *68*, 5492–5493.
(23) Johnson, F. Allylic Strain in Six-Membered Rings. *Chem. Rev.* **1968**, *68*, 375–413.
(24) Koziara, A.; Osowska-Pacewicka, K.; Zawadzki, S.; Zwierzak, A. One-Pot Transformation of Alkyl Bromides into Primary Amines via the Staudinger Reaction. *Synthesis* **1985**, 202–204.
(25) Edwards, M. L.; Snyder, R. D.; Stemerick, D. M. Synthesis and DNA-Binding Properties of Polyamine Analogues. *J. Med. Chem.* **1991**, *34*, 2414–2420.
(26) Cohen, G. M.; Cullis, P. M.; Hartley, J. A.; Mather, A.; Symons, M. C. R.; Wheelhouse, R. T. Targeting of Cytotoxic Agents by Polyamines: Synthesis of a Chlorambucil-Spermidine Conjugate. *J. Chem. Soc., Chem. Commun.* **1992**, 298–300.
(27) Cullis, P. M.; Green, R. E.; Merson-Davies, L.; Travis, N. Probing the Mechanism of Transport and Compartmentalization of Polyamines in Mammalian Cells. *Chem. Biol.* **1999**, *6*, 717–729.
(28) Delcros, J.-G.; Tomasi, S.; Carrington, S.; Martin, B.; Renault, J. Effect of Spermine Conjugation on the Cytotoxicity and Cellular Transport of Acridine. *J. Med. Chem.* **2002**, *45*, 5098–5111.
(29) Wang, C.; Delcros, J.-G.; Biggerstaff, J.; Phanstiel IV, O. Synthesis and Biological Evaluation of N^1-(Anthracen-9-ylmethyl)triamines as Molecular Recognition Elements for the Polyamine Transporter. *J. Med. Chem.* **2003**, *46*, 2663–2671.
(30) Wang, C.; Delcros, J. G.; Biggerstaff, J.; Phanstiel, O., IV Molecular Requirements for Targeting the Polyamine Transport System. Synthesis and Biological Evaluation of Polyamine-Anthracene Conjugates. *J. Med. Chem.* **2003**, *46*, 2672–2682.
(31) Wang, C.; Delcros, J. G.; Cannon, L.; Konate, F.; Carias, H.; Biggerstaff, J.; Gardner, R. A.; Phanstiel IV, O. Defining the Molecular Reqirements for the Selective Delivery of Polyamine-Conjugates into Cells Containing Active Polyamine Transporters. *J. Med. Chem.* **2003**, *46*, 5129–5138.
(32) Wang, L.; Price, H. L.; Juusola, J.; Kline, M.; Phanstiel IV, O. Influence of Polyamine Architecture on the Transport and Topoisomerase II Inhibitory Properties of Polyamine DNA–Intercalator Conjugates. *J. Med. Chem.* **2001**, *44*, 3682–3691.
(33) Pourquier, P.; Takebayashi, Y.; Urasaki, Y.; Gioffre, C.; Kohlhagen, G.; Pommier, Y. Induction of Topoisomerase I Cleavage Complexes by 1-β-Arabinofuranosylcytosine (ara-C) *in vitro* and in Ara-C-treated Cells. *Proc. Natl. Acad. Sci. U.S.A.* **2000**, *97*, 1885–1890.
(34) Pommier, Y.; Fesen, M. R.; Goldwasser, F. Topoisomerase II Inhibitors: the Epipodophyllotoxins, *m*-AMSA, and the Ellipticine Derivatives. *Cancer Chemotherapy and Biotherapy: Principles and Practice*; Lippincott-Raven: Philadelphia, 1996; pp 435–461.
(35) Jayaraman, M.; Fox, B. M.; Hollingshead, M.; Kohlhagen, G.; Pommier, Y.; Cushman, M. Synthesis of New Dihydroindeno-[1,2-*c*]isoquinoline and Indenoisoquinolinium Chloride Topoisomerase I Inhibitors Having High in Vivo Anticancer Activity in the Hollow Fiber Animal Model. *J. Med. Chem.* **2002**, *45*, 242–249.
(36) Birch, A. J.; Jackson, A. H.; Shannon, P. V. R. New Modification of the Pomeranz-Fritsch Isoquinoline Synthesis. *J. Chem. Soc., Perkin Trans. 1* **1974**, 2185–2190.
(37) Jayaraman, M.; Fanwick, P. E.; Cushman, M. Novel Oxidative Transformation of Indenoisoquinolines to Isoquinoline-3-spiro-3-phthalides in the Presence of Osmium Tetroxide and 4-Methylmorpholine *N*-Oxide. *J. Org. Chem.* **1998**, *63*, 5736–5737.
(38) Wang, Z.; Yang, D.; Mohanakrishnan, A. K.; Fanwick, P. E.; Nampoothiri, P.; Hamel, E.; Cushman, M. Synthesis of B-Ring Homologated Estradiol Analogues that Modulate Tubulin Polymerization and Microtubule Stability. *J. Med. Chem.* **2000**, *43*, 2419–2429.

JM040025Z

Available online at www.sciencedirect.com
SCIENCE DIRECT®
ELSEVIER
Cancer Letters 192 (2003) 67–74
CANCER Letters
www.elsevier.com/locate/canlet

A constitutively active ErbB4 mutant inhibits drug-resistant colony formation by the DU-145 and PC-3 human prostate tumor cell lines

Eric E. Williams, Laurie J. Trout, Richard M. Gallo, Sarah E. Pitfield, Ianthe Bryant, Desi J. Penington, David J. Riese II*

Department of Medicinal Chemistry and Molecular Pharmacology, Purdue University School of Pharmacy, 575 Stadium Mall Drive, Room 224D, West Lafayette, IN 47907-1333, USA

Received 30 August 2002; received in revised form 15 November 2002; accepted 18 November 2002

Abstract

ErbB4 (HER4) is a member of the ErbB family of receptor tyrosine kinases, a family that also includes the Epidermal Growth Factor Receptor (EGFR/ErbB1/HER1), Neu/ErbB2/HER2, and ErbB3/HER3. Several groups have hypothesized that signal transduction by the ErbB4 receptor tyrosine kinase is coupled to differentiation, growth arrest, and tumor suppression in mammary and prostate epithelial cells. In this report we demonstrate that a constitutively active ErbB4 mutant inhibits the formation of drug-resistant colonies by the DU-145 and PC-3 human prostate tumor cell lines. This is consistent with our hypothesis that ErbB4 signaling is growth inhibitory and may be coupled to tumor suppression in prostate cells.

Keywords: ErbB4; Receptor tyrosine kinase; Growth inhibition; Tumor suppression; Prostate cancer

1. Introduction

ErbB4 is a member of the ErbB family of receptor tyrosine kinases, a family that also includes the epidermal growth factor (EGF) receptor (EGFR/ErbB1/HER1), ErbB2/HER2/Neu, and ErbB3/HER3 [1–3]. The agonists for these receptors are members of the EGF family of peptide hormones, which includes more than 20 different growth factors (reviewed in [2–4]. The signaling network comprised of these hormones and receptors regulates cell proliferation and differentiation, as well as other cellular functions. Moreover, deregulated signaling by this network, typically due to inappropriate receptor or ligand (over)expression, plays a significant role in many human tumors [3,5–7]. For example, EGFR or ErbB2 overexpression is detected in a significant percentage of human breast tumors and this overexpression correlates with increased metastatic potential, chemoresistance, and poorer patient prognosis.

In contrast, relatively little is known about the roles that ErbB4 plays in tumorigenesis. ErbB4 overexpression is much less common in mammary tumor samples than is EGFR or ErbB2 overexpression. Moreover, ErbB4 overexpression in mammary tumor samples correlates with a more favorable prognosis,

* Corresponding author. Tel.: +1-765-494-6091; fax: +1-765-494-1414.
E-mail address: driese@purdue.edu (D.J. Riese).

0304-3835/02/$ - see front matter © 2002 Elsevier Science Ireland Ltd. All rights reserved.
doi:10.1016/S0304-3835(02)00690-0

not a less favorable prognosis [8–11]. The expression of ErbB4 and its ligands in the developing mouse mammary epithelium is highest late in pregnancy and during lactation, and corresponds with a period of terminal differentiation of the mammary epithelium and only limited proliferation [12,13]. Finally, the normal human prostate epithelium exhibits abundant ErbB4 expression; in contrast, ErbB4 expression has not been detected in any cultured human prostate tumor cell line studied to date [14,15]. These data have led investigators to hypothesize that ErbB4 signaling is coupled to terminal differentiation, growth arrest, and tumor suppression in the mammary and prostate epithelia.

A typical strategy for studying the function of a given ErbB family receptor involves assessing the effect of an EGF family hormone that binds to the ErbB family receptor of interest. These studies can be done either in cells that endogenously express the receptor of interest or in cells that overexpress the appropriate receptor. However, EGF family hormones stimulate heterodimerization of the cognate (binding) ErbB family receptor with any other ErbB family receptor present. This results in tyrosine phosphorylation and signaling by both the cognate ErbB family receptor as well as any other ErbB receptor. Thus, in human breast and prostate tumor cell lines, which frequently express EGFR, ErbB2, and ErbB3, ligands for ErbB4 stimulate not only ErbB4 signaling, but signaling by the other ErbB family receptors as well. Consequently, stimulation with ErbB4 ligands has been of limited value in studying ErbB4 function. Nonetheless, the ErbB4 ligand Neuregulin1beta (NRG1β) stimulates differentiation of mammary epithelium to lobuloalveoli in vivo [16] and stimulates in vitro differentiation of the AU-565 human tumor cell line [17,18]. Furthermore, ErbB4 expression in the SUM102 human mammary tumor cell lines permits the induction of differentiation and growth inhibition by NRG1β [19]. However, efforts by our laboratory to extend these results to other human breast tumor cell lines and to prostate tumor cell lines have failed.

In response, we have embarked on a genetic strategy to study ErbB4 function. We have previously reported the construction of three constitutively active human ErbB4 mutants. These mutants are the result of a single cysteine substitution for Gln646, His647, or Ala648 of the ErbB4 extracellular, juxtamembrane domain. Our initial analyses of these mutants revealed that these mutants, unlike a constitutively active ErbB2 mutant, fail to malignantly transform the growth of rodent fibroblast cell lines [20]. In this report we show that one of these mutants inhibits drug-resistant colony formation by two human prostate tumor cell lines. These data suggest that ErbB4 may indeed be coupled to differentiation, growth arrest, and tumor suppression in the prostate epithelium.

2. Materials and methods

2.1. Cell lines and cell culture

Mouse C127 fibroblasts and the ψ2 and PA317 recombinant retrovirus packaging cell lines are generous gifts of Dr Daniel DiMaio (Yale University, New Haven, Connecticut, USA). These cells were cultured essentially as described previously [21,22]. PC-3 and DU-145 human prostate tumor cell lines were obtained from American Type Culture Collection and were cultured in accordance with vendor recommendations. Cell culture media and supplements were obtained from GIBCO/BRL/Life Technologies. Fetal bovine serum and G418 were obtained from Gemini Bioproducts. Plasticware and Giemsa stain were obtained from Fisher Scientific.

2.2. Retrovirus infections and drug-resistant colony formation assays

Recombinant amphotropic retroviruses were produced essentially as described earlier [22]. Briefly, the recombinant retroviral constructs pLXSN (vector) [23], pLXSN-ErbB4 (ErbB4 WT) [24], pLXSN-ErbB2 V664E (ErbB2*) [25], pLXSN-ErbB4 Q646C, pLXSN-ErbB4 H647C, and pLXSN-ErbB4 A648C [20] were transfected into the ψ2 ecotropic retrovirus packaging cell line [26]. Transfected cells were selected using G418 and drug-resistant colonies were pooled and expanded into stable cell lines. Recombinant ecotropic retroviruses were recovered from the conditioned media of the recombinant ψ2 cell lines. These stocks were used to infect the PA317 amphotropic retrovirus packaging cell line [27].

Infected cells were selected using G418 and drug-resistant colonies were pooled and expanded into stable cell lines. Recombinant amphotropic retroviruses were recovered from the conditioned media of the recombinant PA317 cell lines. pLXSN is a generous gift of Dr Daniel DiMaio (Yale University, New Haven, Connecticut, USA). pLXSN-ErbB2* is a generous gift of Dr Lisa Petti (Albany Medical College, Albany, New York, USA).

C127, DU-145, and PC-3 infections with the recombinant amphotropic retroviruses were performed essentially as described earlier [20–22]. Infected cells were selected using G418. Approximately 12 days after infection, drug-resistant colonies were stained using Giemsa. The tissue culture plates were digitized using an Epson flatbed scanner set for 600 dpi. The digital images were cropped, annotated and combined into composite images. The contrast of the images was enhanced and the background was minimized to maximize the signal–noise ratio. Manipulations of the digital images were performed using Adobe Photoshop.

Drug-resistant colonies were counted manually and the retrovirus titer for each combination of retrovirus and cell line was determined by dividing the number of colonies by the volume of retrovirus used in the infection. The average viral titers were calculated from at least ten independent sets of infections. The efficiency of drug-resistant colony formation was calculated for each retrovirus stock in the DU-145 cell line by dividing the retroviral titers in the DU-145 cells by the corresponding retroviral titers in the C127 cells. These values are expressed as mean percentages calculated from at least ten independent sets of infections. The standard error was also calculated for each mean percentage. Analogous calculations were performed to calculate the efficiency of drug-resistant colony formation for each retrovirus stock in the PC-3 cell lines.

2.3. Immunoprecipitation and immunoblotting

Anti-ErbB4 immunoprecipitations and anti-phosphotyrosine immunoblotting were performed essentially as described earlier [20]. Briefly, C127 cells were starved overnight in serum-free medium, then lysed using an ice-cold isotonic lysis buffer supplemented with the non-ionic detergent NP-40 (Sigma). Nuclei and cellular debris were cleared from the lysates by centrifugation. The protein content of the lysate supernatants was determined using a modified Bradford protein assay (Pierce). ErbB4 was immunoprecipitated from equal amounts of lysate using protein A sepharose (Amersham/Pharmacia) and an anti-ErbB4 rabbit polyclonal antibody (Santa Cruz Biotechnology). The precipitates were washed with an isotonic lysis buffer and the proteins were released from the sepharose beads by boiling in a reducing SDS sample buffer. The samples were resolved by SDS-PAGE using a 7.5% acrylamide gel and were electroblotted onto nitrocellulose. The resulting blot was probed with an anti-phosphotyrosine mouse monoclonal antibody (Upstate Biotechnology). Primary antibody binding was detected and visualized using a goat anti-mouse antibody conjugated to horseradish peroxidase (Pierce) and enhanced chemiluminescence (Amersham/Pharmacia). The chemilumigram was digitized using an Epson flatbed scanner set for 600 dpi resolution. The digital images were cropped and annotated using Adobe Photoshop.

3. Results

3.1. The ErbB4 Q646C mutant inhibits drug-resistant colony formation by the DU-145 human prostate tumor cell line

We previously described the construction and packaging of recombinant retroviral vectors that express the neomycin resistance gene as well as the constitutively active ErbB4 mutants [20]. We infected DU-145 cells with these retroviruses and selected for drug-resistant colonies using G418 to assess whether any of the constitutively active ErbB4 mutants inhibits drug-resistant colony formation. As controls we also infected DU-145 cells with recombinant retroviruses that carry only the neomycin resistance gene (Vector), with recombinant retroviruses that express a constitutively active (V664E) mutant of the rat ErbB2 gene (ErbB2*) [25], and with recombinant retroviruses that express the wild-type ErbB4 gene. To control for differences in absolute viral titers, we infected C127 mouse fibroblasts in parallel and

assayed the formation of drug-resistant colonies of infected cells.

As shown in Fig. 1, DU-145 cells infected with the recombinant retrovirus that expresses the ErbB4 Q646C mutant form fewer drug-resistant colonies than do DU-145 cells infected with the other recombinant retroviruses. Furthermore, the titer of the ErbB4 Q646C recombinant retrovirus in the DU-145 cells is less than the titers of the other recombinant retroviruses (Table 1). However, the titer of the ErbB4 Q646C recombinant retrovirus in C127 fibroblasts is not less than the titer of most of the other recombinant retroviruses (Table 1). Thus, the ratio of the ErbB4 Q646C retroviral titers in DU-145 and C127 cells is much less than the corresponding ratios of the other retrovirus titers (Table 1). Indeed, it appears that the ErbB4 Q646C mutant inhibits drug-resistant colony formation by DU-145 cells by approximately 90%.

3.2. The ErbB4 Q646C mutant inhibits drug-resistant colony formation by the PC-3 human prostate tumor cell line

We infected PC-3 cells in parallel with the DU-145 and C127 infections. The results of these infections

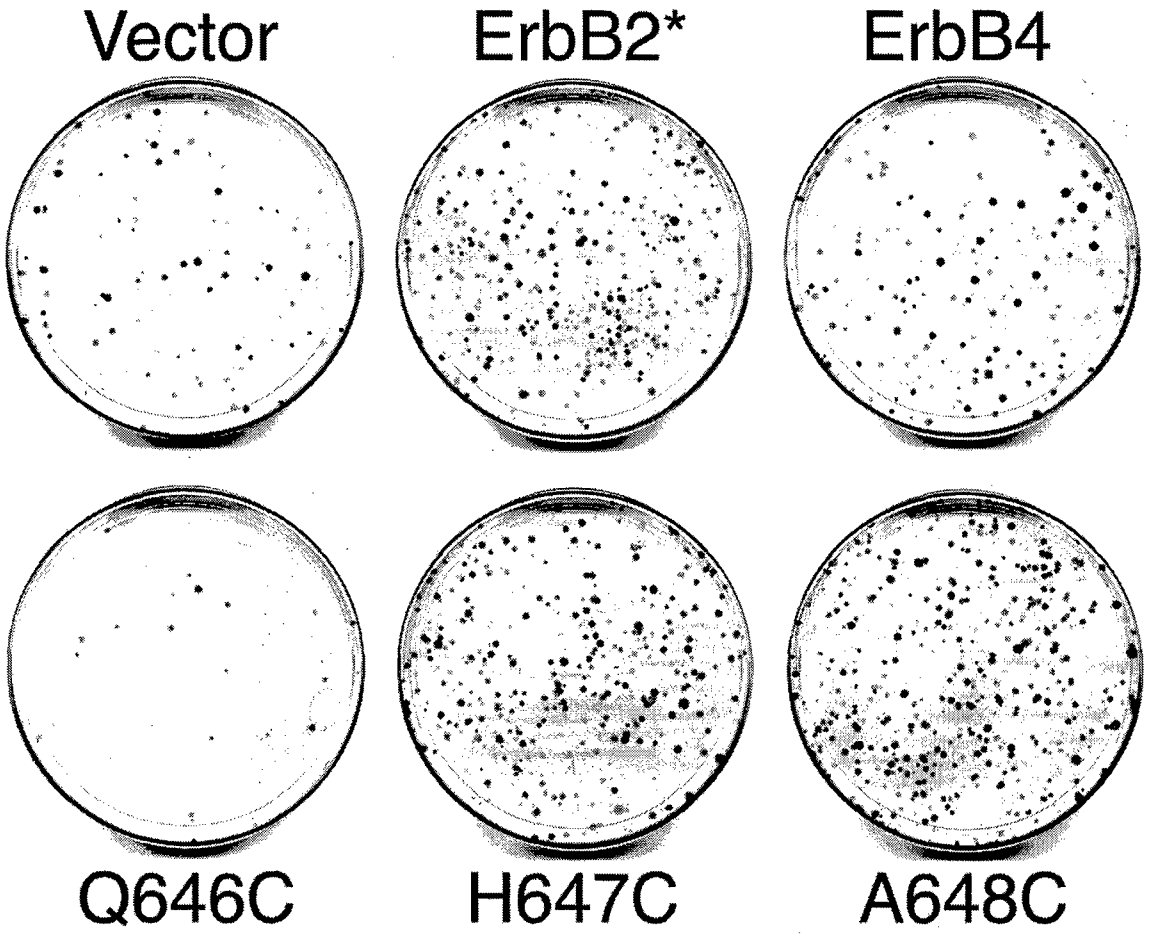

Fig. 1. The ErbB4 Q646C mutant inhibits drug-resistant colony formation by the DU-145 human prostate tumor cell line. DU-145 human prostate cells were infected with recombinant amphotropic retroviruses that carry the neomycin resistance gene (Vector) or with retroviruses that carry the neomycin resistance gene along with a constitutively active ErbB2 mutant (ErbB2*), wild-type ErbB4 (ErbB4), or constitutively active ErbB4 mutants (Q646C, H647C, A648C). Infected cells were selected using 600 μg/ml G418. Colonies of drug-resistant cells were stained using Giemsa and counted.

Table 1
The ErbB4 Q646C mutant specifically inhibits drug-resistant colony formation by the DU-145 and PC-3 human prostate tumor cell lines[a]

	Viral titers			Colony formation efficiency	
Virus	Cell line			Ratios	
Stock	C127	DU-145	PC-3	DU-145/C127	PC-3/C127
Vector	1.14E + 06	7.88E + 04	1.21 E + 05	10.7 ± 2.7	19.4 ± 5.7
ErbB2*	2.92E + 05	3.23E + 04	3.09E + 04	11.9 ± 1.8	15.6 ± 3.9
ErbB4 WT	1.55E + 05	1.44E + 04	2.27E + 04	12.0 ± 3.1	25.3 ± 7.5
Q646C	6.17E + 05	3.42E + 03	1.56E + 04	0.6 ± 0.1	3.1 ± 0.8
H647C	8.65E + 05	4.59E + 04	6.27E + 04	7.2 ± 1.2	17.3 ± 6.3
A648C	1.49E + 05	1.46E + 04	1.67E + 04	11.8 ± 2.1	15.0 ± 2.8

[a] We counted the number of colonies on each plate of infected DU-145, PC-3, and C127 cells and divided by the volume of retrovirus used to infect the cells to determine the titer of each retrovirus stock in each of the three cell lines. To compare the relative efficiency of each retrovirus stock at inducing drug-resistant colony formation in the DU-145 cell line, we divided the titer of each retrovirus stock in the DU-145 cell line by the titer of the same retrovirus stock in the C127 cell line. This value is expressed as a mean percentage calculated from at least ten independent sets of infections. The standard error for each mean was calculated and is reported. We performed analogous calculations to determine the efficiency of drug-resistant colony formation of each retrovirus stock in the PC-3 cell lines.

are similar to the results of the DU-145 infections. PC-3 cells infected with the recombinant retrovirus that expresses the ErbB4 Q646C mutant form fewer drug-resistant colonies than do PC-3 cells infected with the recombinant retroviruses that express the other ErbB4 constructs (Fig. 2). Furthermore, the titer of the ErbB4 Q646C recombinant retrovirus in the PC-3 cells is less than the titers of the other recombinant retroviruses (Table 1). Finally, the ratio of the ErbB4 Q646C retroviral titers in PC-3 and C127 cells is much less than the corresponding ratios of the other retrovirus titers (Table 1). Indeed, it appears that the ErbB4 Q646C mutant inhibits drug-resistant colony formation by PC-3 cells by approximately 75%.

3.3. The constitutively active ErbB4 mutants are expressed and tyrosine phosphorylated in the mouse C127 fibroblast cell line

We were concerned that the failure of the ErbB4 H647C and A648C mutants to inhibit drug-resistant colony formation by the DU-145 and PC-3 human prostate tumor cell lines may be due to an absence of expression and/or tyrosine phosphorylation of these ErbB4 mutants. Consequently, we pooled drug-resistant colonies that resulted from infections of C127 cells and generated stable cell lines. We assayed ErbB4 expression and tyrosine phosphorylation in these cell lines by ErbB4 immunoprecipitation and anti-phosphotyrosine immunoblotting.

In Fig. 3 we show that all three constitutively active ErbB4 mutants are expressed and display ligand-independent tyrosine phosphorylation in the appropriate C127 cell lines. Indeed, it appears that the ErbB4 Q646C mutant exhibits less tyrosine phosphorylation than the ErbB4 H647C and A648C mutants. This suggests that the failure of the ErbB4 H647C and A648C mutants to inhibit drug-resistant colony formation by the DU-145 and PC-3 cell lines is not due to an absence of expression and/or tyrosine phosphorylation of these ErbB4 mutants.

4. Discussion

Here we demonstrate that the Q646C constitutively active ErbB4 mutant inhibits drug-resistant colony formation by the DU-145 and PC-3 human prostate tumor cell lines. This suggests that ErbB4 signaling is coupled to prostate cell growth arrest and tumor suppression. Several issues remain to be resolved in future experiments.

The phenotype that underlies ErbB4 coupling to inhibition of drug resistant colony formation has yet to be determined. For example, it is possible that ErbB4 couples to specific cell cycle arrest. However, it is also possible that ErbB4 is coupling to apoptosis rather than

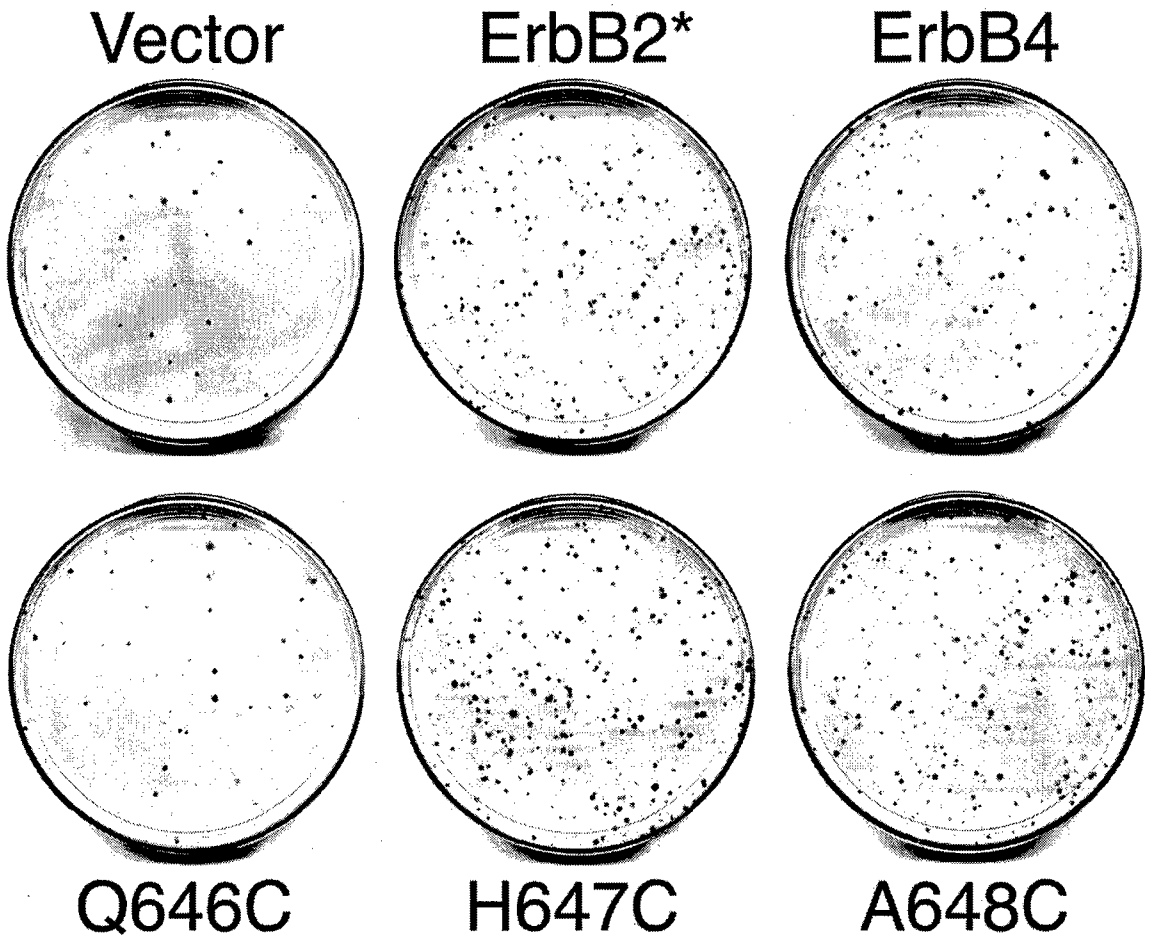

Fig. 2. The ErbB4 Q646C mutant inhibits drug-resistant colony formation by the PC-3 human prostate tumor cell line. PC-3 human prostate cells were infected with recombinant amphotropic retroviruses that carry the neomycin resistance gene (Vector) or with retroviruses that carry the neomycin resistance gene along with a constitutively active ErbB2 mutant (ErbB2*), wild-type ErbB4 (ErbB4), or constitutively active ErbB4 mutants (Q646C, H647C, A648C). Infected cells were selected using 600 μg/ml G418. Colonies of drug-resistant cells were stained using Giemsa and counted.

growth arrest. Since it is impossible to evaluate these hypotheses with the experimental system described in this report, we are developing a conditional expression system that should enable us to determine whether ErbB4 signaling is coupled to cell cycle arrest, apoptosis, or non-specific growth arrest.

Another goal for future experiments is to determine why the Q646C ErbB4 mutant is coupled to inhibition of drug-resistant colony formation by prostate tumor cell lines, whereas the H647C and A648C ErbB4 mutants are not. The differential coupling of these ErbB4 mutants is analogous to the differential coupling of constitutively phosphorylated rat ErbB2 mutants to growth transformation of rodent fibroblasts [28]. It is also analogous to the differential coupling of mutants of the bovine papillomavirus (BPV) E5 protein to malignant growth transformation of rodent fibroblasts. This differential coupling is in marked contrast to the fact that several of these BPV E5 mutants stimulate abundant platelet-derived growth factor receptor tyrosine phosphorylation [29,30]. In both of these examples, it is believed that the constitutively phosphorylated receptor tyrosine kinases are phosphorylated on different individual tyrosine residues, resulting in differential coupling to downstream signaling proteins and biological

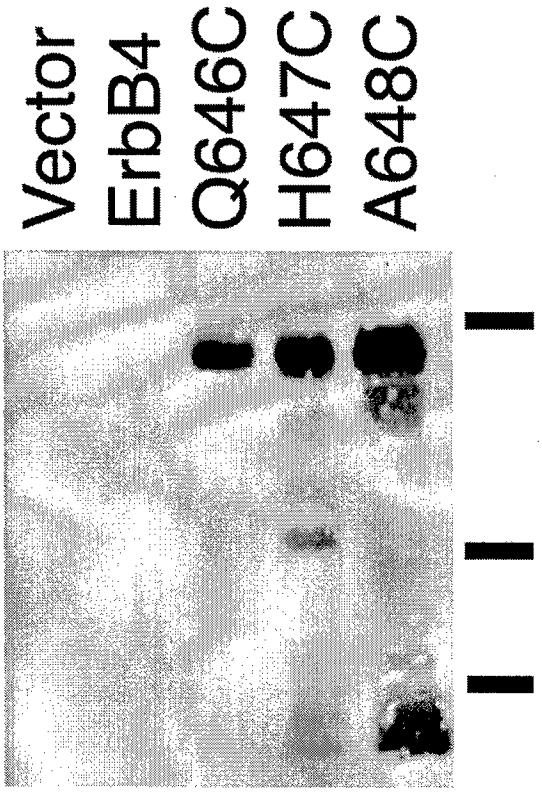

Fig. 3. The constitutively active ErbB4 mutants are expressed and tyrosine phosphorylated in the mouse C127 fibroblast cell line. C127 fibroblasts were infected with recombinant amphotropic retroviruses that express the neomycin resistance gene (Vector) or with retroviruses that express the neomycin resistance gene along with wild-type ErbB4 (ErbB4) or constitutively active ErbB4 mutants (Q646C, H647C, A648C). Infected cells were selected using 1000 μg/ml G418. Colonies of drug-resistant cells were pooled and expanded into stable cell lines. Confluent 100 mm plates of each cell line were incubated in serum-free medium for 24 h, after which cells were lysed. ErbB4 was precipitated using specific antibodies and the precipitates were resolved by SDS-PAGE and electroblotted onto nitrocellulose. The blot was probed with an anti-phosphotyrosine mouse monoclonal antibody. Antibody binding was detected and visualized using a goat anti-mouse secondary antibody coupled to horseradish peroxidase and enhanced chemiluminescence. Bars indicate the positions of the molecular weight markers (198 kDa, 115 kDa, and 93 kDa). Tyrosine phosphorylated ErbB4 is represented by the band with apparent mobility of approximately 190 kDa.

responses. Indeed, different ErbB4 ligands cause different patterns of ErbB4 phosphorylation and differential coupling to downstream signaling effectors and biological responses [31]. Thus, we hypothesize that the functional differences between the ErbB4 Q646C mutant and the other constitutively active ErbB4 mutants are due to phosphorylation on different ErbB4 tyrosine residues. Mapping the sites of ErbB4 tyrosine phosphorylation for the three constitutively active ErbB4 mutants and genetic studies to identify the sites of ErbB4 tyrosine phosphorylation that couple ErbB4 to inhibition of drug resistant colony formation will enable us to formally address this hypothesis.

Finally, additional experiments will be necessary to formally test the hypothesis that ErbB4 is a prostate tumor suppressor. Male transgenic mice that exhibit tissue specific ectopic expression of the Q646C ErbB4 mutant in the prostate gland would be an appropriate in vivo model system for assessing whether constitutive ErbB4 signaling is sufficient to suppress prostate tumorigenesis.

Acknowledgements

E.E.W. was supported by an undergraduate research fellowship from the American Association of Colleges of Pharmacy and Merck. L.J.T. was supported by an undergraduate research training grant from the US Army Medical Research and Materiel Command (DAMD17-02-1-0555). R.M.G. was supported by a Purdue University Andrews Fellowship. I.B. was supported by a Howard Hughes Medical Institute undergraduate research fellowship, a MARC/AIM summer undergraduate research fellowship, and a summer undergraduate research fellowship from the American Society for Microbiology. D.J.P. was supported by a Purdue University Graduate Opportunities Fellowship. We also acknowledge additional support from the US Army Medical Research and Materiel Command (DAMD17-00-1-0415, DAMD17-00-1-0416, and DAMD17-02-1-0130 to D.J.R.), the Indiana Elks Foundation (to D.J.R.), and the American Cancer Society (IRG-58-006 to the Purdue Cancer Center).

References

[1] J. Schlessinger, Cell signaling by receptor tyrosine kinases, Cell 103 (2000) 211–225.

[2] W.J. Gullick, The type I growth factor receptors and their ligands considered as a complex system, Endocrine-Related Cancer 8 (2001) 75–82.
[3] Y. Yarden, M.X. Sliwkowski, Untangling the ErbB signalling network, Nat. Rev. Mol. Cell Biol. 2 (2001) 127–137.
[4] R. Kumar, R.K. Vadlamudi, The EGF family of growth factors, J. Clin. Ligand Assay 23 (2001) 233–237.
[5] D.F. Stern, Tyrosine kinase signalling in breast cancer: ErbB family receptor tyrosine kinases, Breast Cancer Res. 2 (2000) 176–183.
[6] N. Normanno, C. Bianco, A. DeLuca, D.S. Salomon, The role of EGF-related peptides in tumor growth, Frontiers Biosci. 6 (2001) d685–d707.
[7] F. Ozawa, H. Friess, A. Tempia-Caliera, J. Kleeff, M.W. Buchler, Growth factors and their receptors in pancreatic cancer, Teratogen. Carcinogen. Mutagen. 21 (2001) 27–44.
[8] S.S. Bacus, D. Chin, Y. Yarden, C.R. Zelnick, D.F. Stern, Type 1 receptor tyrosine kinases are differentially phosphorylated in mammary carcinoma and differentially associated with steroid receptors, Am. J. Pathol. 148 (1996) 549–558.
[9] J.M. Knowlden, J.W. Gee, L.T. Seery, L. Farrow, W.J. Gullick, I.O. Ellis, R.W. Blamey, J.R. Robertson, R.I. Nicholson, c-ErbB3 and c-ErbB4 expression is a feature of the endocrine responsive phenotype in clinical cancer, Oncogene 17 (1998) 1949–1957.
[10] V. Pawlowski, F. Revillion, M. Hebbar, L. Hornez, J-P. Peyrat, Prognostic value of the type I growth factor receptors in a large series of human primary breast cancers quantified with a real-time reverse transcription-polymerase chain reaction assay, Clin. Cancer Res. 6 (2000) 4217–4225.
[11] Z. Suo, B. Risberg, M.G. Kaisson, K. Willman, A. Tierens, E. Skovlund, J.M. Nesland, EGFR family expression in breast carcinomas, c-erbB2 and c-erbB4 receptors have different effects on survival, J. Pathol. 196 (2002) 17–25.
[12] J.A. Schroeder, D.C. Lee, Dynamic expression and activation of ErbB receptors in the developing mouse mammary gland, Cell Growth Differ. 9 (1998) 451–464.
[13] K.L. Troyer, D.C. Lee, Regulation of mammary gland development and tumorigenesis by the ErbB signaling network, J. Mammary Gland Biol. Neoplasia 6 (2001) 7–21.
[14] D. Robinson, F. He, T. Pretlow, H-J. Kung, A tyrosine kinase profile of prostate carcinoma, Proc. Natl. Acad. Sci. USA 93 (1996) 5958–5962.
[15] A.W. Grasso, D. Wen, C.M. Miller, J.S. Rhim, T.G. Pretlow, H.-J. Kung, ErbB kinases and NDF signaling in human prostate cancer cells, Oncogene 15 (1997) 2705–2716.
[16] F.E. Jones, D.J. Jerry, B.C. Guarino, G.C. Andrews, D.F. Stern, Heregulin induces in vivo proliferation and differentiation of mammary epithelium into secretory lobuloalveoli, Cell Growth Differ. 7 (1995) 1031–1038.
[17] E. Peles, S.S. Bacus, R.A. Koski, H.S. Lu, D. Wen, S.G. Ogden, R. Ben Levy, Y. Yarden, Isolation of the Neu/HER-2 stimulatory ligand: a 44 kd glycoprotein that induces differentiation of mammary tumor cells, Cell 69 (1992) 205–216.
[18] D. Wen, E. Peles, R. Cupples, S.V. Suggs, S.S. Bacus, Y. Luo, G. Trail, S. Hu, S.M. Silbiger, R. Ben Levy, R.A. Koski, H.S. Lu, Y. Yarden, Neu differentiation factor: a transmembrane glycoprotein containing an EGF domain and an immunoglobulin homology unit, Cell 69 (1992) 559–572.
[19] C.I. Sartor, H. Zhou, E. Kozlowska, K. Guttridge, E. Kawata, L. Caskey, J. Harrelson, N. Hynes, S. Ethier, B. Calvo, H.S. Earp III, HER4 mediates ligand-dependent antiproliferative and differentiation responses in human breast cancer cells, Mol. Cell Biol. 21 (2001) 4265–4275.
[20] D.J. Penington, I. Bryant, D.J. Riese II, Constitutively active ErbB4 and ErbB2 mutants exhibit distinct biological activities, Cell Growth Differ. 13 (2002) 247–256.
[21] D.J. Riese II, D. DiMaio, An intact PDGF signaling pathway is required for efficient growth transformation of mouse C127 cells by the bovine papillomavirus E5 protein, Oncogene 10 (1995) 1431–1439.
[22] C. Leptak, S. Ramon y Cajal, R. Kulke, B.H. Horwitz, D.J. Riese, G.P. Dotto, D. DiMaio, Tumorigenic transformation of murine keratinocytes by the E5 genes of bovine papillomavirus type 1 and human papillomavirus type 16, J. Virol. 65 (1991) 7078–7083.
[23] D.A. Miller, G.J. Rosman, Improved retroviral vectors for gene transfer and expression, BioTechniques 7 (1989) 980–990.
[24] D.J. Riese II, T.M. Van Raaij, G.D. Plowman, G.C. Andrews, D.F. Stern, The cellular response to neuregulins is governed by complex interactions of the ErbB receptor family, Mol. Cell Biol. 15 (1995) 5770–5776.
[25] L.M. Petti, F.A. Ray, Transformation of mortal human fibroblasts and activation of a growth inhibitory pathway by the bovine papillomavirus E5 oncoprotein, Cell Growth Differ. 11 (2000) 395–408.
[26] R. Mann, R.C. Mulligan, D. Baltimore, Construction of a retrovirus packaging mutant and its use to produce helper-free defective retrovirus, Cell 33 (1983) 153–159.
[27] D.A. Muller, C. Buttimore, Redesign of retrovirus packaging cell lines to avoid recombination leading to helper virus production, Mol. Cell Biol. 6 (1986) 2895–2902.
[28] C.L. Burke, D.F. Stern, Activation of Neu (ErbB2) mediated by disulfide bond-induced dimerization reveals a receptor tyrosine kinase dimer interface, Mol. Cell Biol. 18 (1998) 5371–5379.
[29] L.A. Nilson, R.A. Gottlieb, G.W. Pollack, D. DiMaio, Mutational analysis of the interaction between the bovine papillomavirus E5 transforming protein and the endogenous β receptor for platelet derived growth factor, J. Virol. 72 (1998) 5869–5874.
[30] O. Klein, G.W. Pollack, T. Surti, D. Kegler-Ebo, S.O. Smith, D. DiMaio, Role of glutamine 17 of the bovine papillomavirus E5 protein in platelet-derived growth factor β receptor activation and cell transformation, J. Virol. 72 (1998) 8921–8932.
[31] C. Sweeney, C. Lai, D.J. Riese II, A.J. Diamonti, L.C. Cantley, K.L. Carraway III, Ligand Discrimination in Signaling through an ErbB4 Receptor Homodimer, J. Biol. Chem. 276 (2000) 19803–19807.